

# Harnessing Simulation for Molecular Embeddings

Christopher Fifty<sup>\*1</sup> Joseph M. Paggi<sup>\*1</sup> Ehsan Amid<sup>2</sup> Jure Leskovec<sup>1</sup> Ron Dror<sup>1</sup>

## Abstract

While deep learning has unlocked advances in computational biology once thought to be decades away, extending deep learning techniques to the molecular domain has proven challenging, as labeled data is scarce and the benefit from self-supervised learning can be negligible in many cases. In this work, we explore a different approach. Inspired by methods in deep reinforcement learning and robotics, we explore harnessing physics-based molecular simulation to develop molecular embeddings. By fitting a Graph Neural Network to simulation data, molecules that display similar interactions with biological targets under simulation develop similar representations in the embedding space. These embeddings can then be used to initialize the feature space of down-stream models trained on real-world data to encode information learned during simulation into a molecular prediction task. Our experimental findings indicate this approach improves the performance of existing deep learning models on real-world molecular prediction tasks by as much as 38% with minimal modification to the down-stream model and no hyperparameter tuning.

## 1. Introduction

Most drugs are small molecules that act by binding to a target protein, thereby influencing its function. Researchers often identify a protein or other biological target associated with an ailment and try to find small molecules that inhibit or stimulate said target. While machine learning has been used to predict molecule-target interactions — specifically, given an input molecule, predict the extent to which it will activate or inhibit a biological target — many approaches are challenged by the paucity of labeled data relating to any one given target. Moreover, the behavior across targets can vary greatly due to significantly different binding geometries and structures.

Determining the ground-truth interaction of a small molecule with a biological target may involve a lengthy period of cell cultivation followed by a multi-step biological assay requiring specialized equipment. The throughput of these assays is limited, and synthesizing molecules to be tested is expensive. As a result, supervised datasets measuring the interactions between small molecules and a biological target often contain on the order of 10s or 100s of data points.

To cope with the scarcity of labeled data, significant work has focused on developing few-shot learning algorithms endowed with inductive biases suited towards molecular machine learning (Schimunek et al., 2022; Chen et al., 2022) or creating increasingly clever self-supervised training objectives to learn context-dependent molecular representations from unlabeled data (Wu et al., 2021). However, Sun (2022) finds self-supervised pretraining for molecular prediction tasks often conveys negligible improvement, while incorporating prior knowledge into few-shot learning paradigms can be difficult to implement and/or circumscribed by assumptions specific to a given dataset. In this work, we explore an alternative path — training in simulation.

The past five decades have seen intensive development of physics-based “docking” simulations<sup>1</sup> for predicting whether a small molecule will bind to a given target protein. To bind, the small molecule must have the capacity to (1) adopt a 3D shape complementary to the geometry of the binding site and (2) have characteristics amenable to the receptor (similar hydrophobicity, correct electrical charge, etc.). Physics-based simulations sample many potential 3D structures of the molecule and evaluate the extent to which each shape would bind to the target using physics-based energy functions that capture key properties of real-world molecule-target interactions.

But the most salient feature relates to their capacity to generate near-unlimited labeled data. In contrast to the available

<sup>\*</sup>Equal contribution <sup>1</sup>Stanford University <sup>2</sup>Google Brain. Correspondence to: Christopher Fifty <fifty@cs.stanford.edu>.

<sup>1</sup>The “docking” methods used here are distinct from molecular dynamics (MD) simulations, which simulate the time evolution of a molecular system. MD simulations are difficult to use for predicting binding affinities, as molecules binding to and dissociating from proteins typically occurs on inaccessibly long time scales. Strategies utilizing shorter MD simulations exist (Wang et al., 2015), but these are still too computationally intensive and require careful setup for each target.

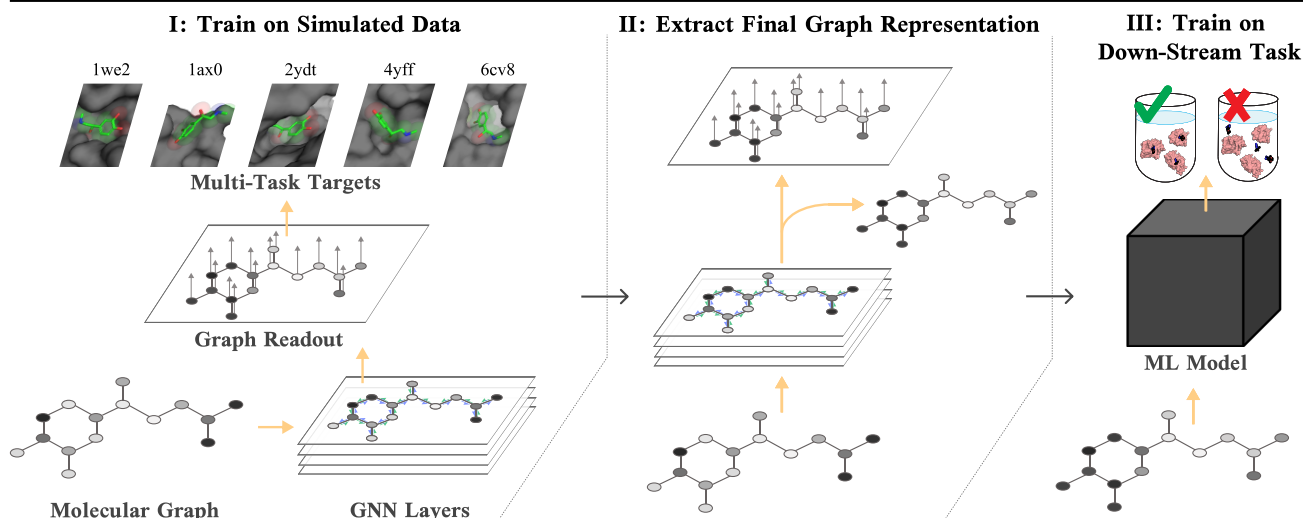


**Figure 1.** The end-to-end paradigm of training on molecular simulation data: (I) train a multi-task GNN to map a small molecule to binding energies (kcal/mol) determined by the interactions between this small molecule and protein targets in simulation. (II) extract the pre-readout graph representation. (III) for a downstream task, replace the default feature space with the learned molecular embeddings. The multi-task targets 1we2, 1ax0, 2ydt, 4yff, and 6cv8, represent Protein Data Bank codes for 5 of the 2,034 targets in our actual dataset.

supervised datasets, which contain 10s or 100s of examples per biological target, we can measure 1000s, 10,000s, or even 100,000s of interactions per target in simulation. Moreover, we can repeat this process across many different protein targets, thereby measuring how a collection of small molecules interact across a diverse range of targets.

While simulation can convey useful information regarding the interactions between molecules and targets, it applies the same set of computations to each molecular interaction and is unable to learn from new evidence. Deep learning is, in many respects, the opposite. It makes minimal assumptions but requires significant quantities of labeled data to learn an effective mapping from example to label. The confluence of both may present a solution.

In this work, we explore encoding molecular representations learned during simulation into downstream applications of molecular prediction tasks. Our approach begins by training an MPNN (Gilmer et al., 2017) on a multi-task dataset composed of several thousand biological targets, each with 1000s of datapoints corresponding to how various small molecules interact with this target in simulation. We then export the final graph representation as a molecular embedding that can be used as a starting point to train on a down-stream molecular prediction task. Our experimental findings indicate this approach may significantly improve performance, especially in few-shot learning settings.

## 2. Related Works

Simulating reality with computational approximations presents an avenue to generate data for deep learning systems that model real-world phenomena. Such an approach has been thoroughly explored and leveraged in the field

of deep reinforcement learning and robotics, as collecting real-world data of an agent’s actions often entails the setup of a physical robotic apparatus, followed by hundreds or thousands of hours of monitoring a trial-and-error learning process (Tobin et al., 2017; Kalashnikov et al., 2018; Brohan et al., 2022). While seemingly dissimilar from molecular machine learning, both modalities are challenged by a dearth of supervised training data. Moreover, collecting new data is expensive, requiring specialized equipment, facilities, and personnel. In this sense, both modalities are similar, and some of the solutions developed for deep reinforcement learning may transfer to molecular machine learning.

A non-trivial gap often manifests between a policy learned in simulation and applying said policy to the real world — commonly referred to as the sim2real gap. Innovations in this domain have led to policies learned entirely in simulation transferring to real-world tasks such as autonomous drone flight (Sadeghi & Levine, 2016) and quadroped robotic locomotion (Tan et al., 2018). Our work adopts a similar approach by encoding the interactions between small molecules and protein targets during simulation into molecular embeddings. We then train a new model above these embeddings to both fit a downstream molecular prediction task and minimize the sim2real gap. To the best of our knowledge, this work may represent the first study of transferring information learned from physics-based molecular simulation to real-world molecular property prediction with deep learning.

While leveraging simulation to benefit molecular property prediction in deep learning paradigms has been largely unexplored, significant effort has been devoted to addressing challenges associated with training deep learning models on small-scale molecular property prediction datasets. We

partition these efforts into two collections. The first relates to developing new training objectives for self-supervision, while the second focuses on incorporating desirable domain-specific inductive biases in the learning process.

Self-supervised training approaches often aim to learn fundamental representations of small molecules sans labeled data. Many techniques apply a variation of atom, subgraph, or structural motif level masking and reconstruction (Hu et al., 2019; Ahmad et al., 2022; Maziarka et al., 2020; Rong et al., 2020), while others begin to incorporate spatial information into molecular graphs to predict the distances among atoms (Zaidi et al., 2022; Fang et al., 2021; Li et al., 2022; Jiao et al., 2022). Still yet others adopt ideas from contrastive learning: creating augmented views of molecular graphs and then learning graphical representations so that the similarity between different views of the same molecule is maximized while the similarity between views of different molecules is minimized (You et al., 2020; Zhu et al., 2021; Hassani & Khasahmadi, 2020; Wu et al., 2021). However, Sun (2022) finds self-supervised pre-training often conveys a negligible benefit and suggest much of the improvement attributed to self-supervised methods may be derived from extensive hyperparameter tuning of downstream tasks rather than the pre-training strategy itself.

A second perspective focuses on enhancing few-shot learning methodologies with inductive biases desirable for molecular machine learning. Wang et al. (2021) propose using a molecule relation graph to improve few-shot learning performance. Schimunek et al. (2022) encode context into molecular representations by querying Modern Hopfield Networks to replace a molecule’s representation with that of an associated context molecule, and Chen et al. (2022) augment molecular meta-learning with an adaptive kernel fitting framework. Finally, Stanley et al. (2021) adapts conventional few-shot learning baselines such as multi-task learning (Caruana, 1997), model-agnostic meta-learning (Finn et al., 2017), and prototypical networks (Snell et al., 2017) to a robust few-shot learning molecular property prediction benchmark. Our findings in section 5 suggest our approach may be complementary to these methods, simply transforming the feature space upon which they operate to the embedding space learned in simulation.

### 3. Approach

Our approach to distill biophysics knowledge from physics-based simulation and encode it into deep learning paradigms is straightforward and visualized in Figure 1. (I) train a multi-task GNN to map a small molecule to binding energies (kcal/mol) determined by the interactions between this small molecule and protein targets in simulation. (II) extract the pre-readout graph representation. (III) for a downstream task, replace the default feature space with the

learned molecular embeddings.

In the following sections, we detail the motivation behind and preparation of our simulation dataset as well as the multi-task training paradigm used to learn molecular embeddings.

**Motivation and Preparation of Simulation Dataset.** To transfer knowledge learned from molecular simulation to real-world property prediction, it is imperative to consider the association between examples and labels learned during simulation, and how that association may transfer to real-world tasks. Under this lens, we observe that 3D conformations – the 3D structures small molecules may adopt when binding to a particular target – may be important in real-world molecular property prediction. However the space of possible 3D conformations a given molecule may adopt is infinite, and many machine learning models operate on 2D chemical structure rather than 3D conformations. Accordingly, we endeavor to abstract this notion of energetically favorable conformations often adopted by a molecule by simulating the extent to which a molecule may bind to many different targets.

To this end, we use Glide, a physics-based docking program (Friesner et al., 2004). Given the 2D structure of a small molecule and the 3D structure of a target protein, Glide considers many potential “poses” (i.e., potential 3D structures of the small molecule bound to the protein), estimates the energetic favorability of each pose using a physics-based scoring function, and returns a predicted affinity based on the most energetically favorable pose. Glide typically ranks strongly in comparative assessments of small molecule–target binding affinity estimation and is widely used across industry and academia (Wang et al., 2016).

We now offer a description of our simulation dataset grounded in comparison to the large-scale, few-shot learning dataset FS-Mol (Stanley et al., 2021). FS-Mol includes a total of 233,786 small molecules and 5135 biological targets, but it includes measured affinities for an average of only 94 small molecules per biological target. Many real-world molecular datasets follow a similar pattern of very few available data points per target. In contrast, physics-based docking simulation can easily explore arbitrarily many small molecule–target interactions. Our simulation dataset contains 32,547 unique small molecules and evaluates, on average, 1601 interactions per target across 2034 protein targets drawn from PDBBind 2020 (Wang et al., 2004). It occupies 77 GB on disk, representing a 16-fold increase over the size of FS-Mol.

**Multi-Task Learning Paradigm.** The simulation dataset naturally induces a multi-task learning paradigm where each protein target represents a separate task. In this way, we map each small molecule to a binding energy (kcal/mol)

determined by the physical interactions this small molecule forms with a protein target during simulation. This process is then repeated across many different protein targets for each small molecule to compose a multi-task learning dataset.

We fit the mapping of a small molecule to simulation-derived binding energies with a 10-layer MPNN augmented with PNA (Corso et al., 2020) and using a graph readout composed of an element-wise maximum, learned weighted sum, and learned weighted mean. The post-readout molecular representation is then passed through a shallow MLP shared among all tasks before using a task-specific projection layer to predict the binding energy for a given target. The model’s parameters are updated with Adam (Kingma & Ba, 2014) to minimize the mean squared error between the model’s predictions and the free energy measurements.

We randomly split our simulation data into 80% train and 20% validation, and use early stopping with a window size of 10 epochs on the validation dataset. Training spans 100 epochs, and the best model checkpoint is loaded from disk. We can then transform the feature space of a downstream molecular prediction dataset to the embedding space by simply making a forward pass through the simulation model, extracting the pre-readout molecular representation, and overwriting the default feature space on disk with the learned representations.

## 4. Embedding Analysis

Our analysis commences with an exploration of the embedding space learned by our model on simulation data. In particular, we analyze the extent to which similarity among the learned molecular embeddings agrees with the implicit notion of similarity defined by physics-based docking simulation. Later, we examine two molecules with dissimilar chemical structures but a tendency to adopt similar 3D conformations when binding to biological targets.

### 4.1. Embedding Space Analysis

While our MPNN model may fit the simulation data, it is unclear if relevant physics-based knowledge is actually encoded into the learned embeddings. Answering this question is the focus of our embedding space analysis.

**Defining Molecular Similarity.** We present 3 ways to measure molecular similarity: physics-based, embedding-based, and fingerprint-based.

Physics-based docking software implicitly encodes a notion of similarity among small molecules. For instance, one may define “similar” small molecules as those that manifest similar binding affinities across many different protein targets; such molecules typically adopt similar 3D conformations

and form similar chemical interactions with targets. We quantify the implicitly defined similarity between a pair of molecules  $m_1, m_2$  in simulation as the relative difference in docking scores across all targets:

$$d(m_1, m_2) = \sum_{t \in \text{targets}} \frac{|t(m_1) - t(m_2)|}{\max_m \{t(m)\} - \min_m \{t(m)\}}. \quad (1)$$

We compute the relative difference in docking score as opposed to the absolute difference as different targets have different ranges of binding affinities, and we wish to avoid lending more weight to targets with larger ranges than to targets with smaller ranges.

Next we define the distance between molecules in the embedding space. Our MPNN embedding model uses a combined graph readout composed of an element-wise max, learned weighted sums, and learned weighted means. Applying any of these pooling operations to the graph embeddings will output a component of the vector used to predict the docking scores associated with this target. Accordingly, we choose the simplest operation — element-wise max pooling — to motivate the distance between two arbitrary molecules in our embedding space.

Let  $m_1, m_2$  be two molecules parameterized by a per-node, learned feature matrix and an adjacency matrix in the embedding space:  $m_1^{(e)} = (\mathcal{V}_1^{(e)}, \mathcal{E}_1^{(e)})$ . We define  $\rho$  to be the max-pooling operation across the embedding dimension for all nodes in the graph.

$$\text{For node embeddings } \mathcal{V}^{(e)} = \begin{bmatrix} v_{1,1} & \dots & v_{1,d} \\ \dots & & \\ v_{n,1} & \dots & v_{n,d} \end{bmatrix} \in \mathbb{R}^{n \times d},$$

$$\rho(\mathcal{V}^{(e)}) \in \mathbb{R}^d, \text{ where } [\rho(\mathcal{V}^{(e)})]_j = \max_i v_{ij}.$$

We can now define the distance between two molecules in the embedding space as the  $l_2$  norm of their element-wise maximum difference:

$$d_\rho(m_1, m_2) = \|\rho(\mathcal{V}_1) - \rho(\mathcal{V}_2)\|_2 \quad (2)$$

One may also apply Equation 2 to the initial feature space used as input to the model:  $m_1^{(f)} = (\mathcal{V}_1^{(f)}, \mathcal{E}_1^{(f)})$ . A model’s feature space is simply the initial numerical representation of a molecule. Machine learning models often define an atom-level feature space as a numerical vector encoding an atom’s element type atomic charge, atomic mass, valency and/or other atomic-level quantities.

A third metric of the distance between two molecules is the Tanimoto distance  $d_\tau$  between their extended-connectivity fingerprints (ECFPs). An ECFP is a binary string indicating whether or not each of many 2D chemical substructures



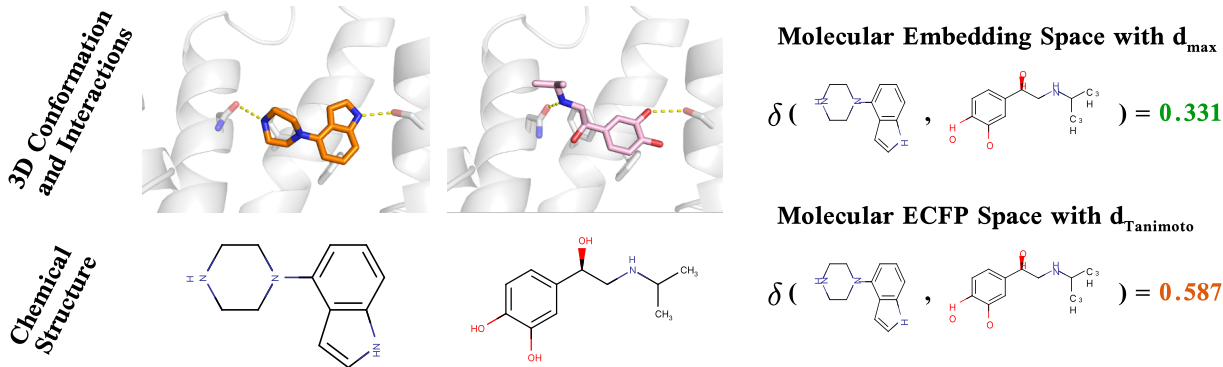


Figure 2. While these two molecules have very different 2D structures, they can adopt similar 3D conformations and form similar interactions with a target protein. Shown are renderings of these molecules in complex with the  $\beta_1$ -adrenergic receptor, with dashed yellow lines indicating hydrogen bonds. These molecules are relatively close in the embedding space, falling in the 33rd percentile amongst a randomly selected set of molecules, as compared to the 58th percentile using the Tanimoto coefficient.

Table 1. Kendall Tau Analysis. Scores are averaged across 100 randomly selected small molecules. The number of swaps indicates the average number of swaps made by KT to transform an ordering to the physics-based ordering. Normalized KT is the number of swaps divided by the number of molecules in an ordering.

	# Swaps ( $\downarrow$ )	Normalized KT ( $\downarrow$ )
Physics	0	0
Embedding $d_\rho$	$2.96 \times 10^7$	0.386
Feature $d_\rho$	$3.73 \times 10^7$	0.488
Tanimoto	$3.28 \times 10^7$	0.429
Random	$3.83 \times 10^7$	0.50

is present in a given molecule. This Tanimoto distance—which is one of the most commonly used notions of molecular similarity in both academia and industry (Rogers & Hahn, 2010)—is defined as the number of chemical sub-structures shared between a pair of molecules divided by the total number of chemical sub-structures present in either molecule. A high value indicates that a pair of molecules share the same components but does not necessarily indicate that those components are connected to one another in the same way or positioned similarly in 3D.

**Comparing Across Metrics.** While one may define various metrics to determine the distance among molecules within a metric space, comparing distances across metric spaces is more involved. One may abstract the notion of distance between two pairs of molecules to an ordering of all molecules ranked by distance to a single molecule. By ranking the similarity of all molecules to an anchor molecule according to one metric, we may quantify the extent to which other metrics produce a (dis)similar ordering with respect to this same molecule. We employ the Kendall Tau rank distance (Kendall, 2004), also known as the bubble-sort distance, to quantify how similar one ranking of molecular similarity is to the physics-based ordering induced by Equation 1

$$K_d(\tau_1, \tau_2) = |\{(i, j) : i < j, [\tau_1(i) \wedge \tau_2(i) > \tau_2(j)] \vee [\tau_1(i) > \tau_1(j) \wedge \tau_2(i) < \tau_2(j)]\}|$$

where  $\tau_1(i)$  and  $\tau_2(i)$  are the rankings of molecule  $i$  given by the rankings  $\tau_1$  and  $\tau_2$ , respectively. Intuitively, this measure counts the number of swaps made during a bubble sort to convert the ordering in the embedding space, feature space, or ECFP space to the ordering in the physics space. As  $\{t | t \in \tau_1\} = \{t | t \in \tau_2\}$ , Kendall Tau satisfies the properties of a metric.

**Findings.** As comparing the product space of  $(32,547 \times 32,547)$  pairs of molecules exceeds our computational resources, we randomly sample 100 small molecules from our dataset to compare the orderings induced by  $d_\rho$  on the embedding space,  $d_\rho$  on the feature space, and Tanimoto distance on the ECFP space with the “ground-truth” orderings induced by Equation 1.

Our findings are summarized in Table 1 and indicate ranking molecules by distance in the embedding space is most similar to the rankings induced by distance in the physics space. Rankings ordered by Tanimoto distance require, on average, 4.5 million more swaps per molecule than orderings sorted by the distance in the embedding space. Similarly, applying  $d_\rho$  in the feature space requires, on average, 77 million more swaps than orderings derived by applying  $d_\rho$  in the embedding space. Random represents a randomly ranked list of molecules and requires an expected, on average 87 million additional swaps per molecule when compared with the embedding ordering.

## 4.2. Visualized Example

To supplement our aggregate analysis, we provide an example of two small molecules that have dissimilar 2D chemical

structures, but are known to adopt similar 3D conformations when binding to targets. We select ChEMBL200234 and levisoprenaline as the small molecules and the  $\beta_1$ -adrenergic receptor (B1AR) as the protein target. While these two molecules are chemically very different, as seen in Figure 2, examining the experimentally determined structure of each one bound to B1AR reveals they adopt similar 3D conformations and form similar chemical interactions (e.g., hydrogen bonds) with the target.

It would be expected that Tanimoto distance determines a low similarity between these two molecules given their disparate chemical structures, but has this type of “binding similarity” been encoded into the molecular embeddings learned from simulation data?

To rigorously answer this question, we randomly sample 100,000 small molecules and order all 100,002 small molecules (the 100,000 randomly sampled molecules + ChEMBL200234 and levisoprenaline) with respect to distance from ChEMBL200234 as well as levisoprenaline. We then extract and average the index of levisoprenaline in the ranked list of ChEMBL200234 and the index of ChEMBL200234 in the ranked list of levisoprenaline to determine a combined score.

Under Tanimoto distance, ChEMBL200234 places levisoprenaline at position 50,204 while levisoprenaline places ChEMBL200234 at position 67,119. In contrast, under the embeddings distance, ChEMBL200234 places levisoprenaline at position 31,650 while levisoprenaline places ChEMBL200234 at position 34,551. This example illustrates that molecules even with dissimilar chemical structures may be placed relatively close to one another in the embedding space, lending support to the hypothesis that the simulation-derived molecular embeddings may encode information about the 3D conformations a molecule may adopt when binding to a target.

## 5. Experiments and Discussion

In our experimental analysis, we seek to answer a simple question: can molecular embeddings that are learned from physics-based simulation improve molecular property prediction?

To this end, we evaluate the simulation-derived molecular embeddings on FS-Mol (Stanley et al., 2021), a few-shot learning dataset designed to reflect the size and scope of datasets used in real-world drug discovery, as well as 10 datasets from the ever-popular MoleculeNet benchmark (Wu et al., 2018). We build our analysis on two conditions reflecting the constraints often imposed on academia and industry where existing models are likely to run efficiently but a capacity — both human and computational — to implement new methods and tune them is limited:

- **Model Agnostic:** the learned embeddings should be applicable and effective across a diverse range of architectures and learning algorithms.
- **Minimal Modification:** replacing the feature space with the simulation-derived embedding space should be effective with minimal modification or hyperparameter tuning.

Table 2. Multi-Task (MT) test  $\Delta$ AUPRC averaged across all targets on FS-Mol.  $\Delta$ AUPRC is an evaluation metric defined in (Stanley et al., 2021) that measures the change in the area under the precision-recall curve over the random classifier baseline. Performance of MT cited from the FS-Mol paper, and EMB-MT indicates the performance of MT when trained on molecular representations in the embedding space rather than the default feature space.

Support Size	MT ( $\uparrow$ )	EMB-MT ( $\uparrow$ )	% increase
16	0.117	0.162	$\Delta 38\%$
32	0.149	0.168	$\Delta 32\%$
64	0.181	0.226	$\Delta 25\%$
128	0.228	0.264	$\Delta 16\%$
256	0.242	0.285	$\Delta 18\%$

**FS-Mol Description.** FS-Mol is a benchmark for few-shot prediction of the activity of small molecules at target proteins. The dataset consists of many individual datasets, each of which corresponds to the measured activities of various small molecules at a particular target protein. These measurements were transcribed from scientific papers reporting the results of biological assays physically performed in laboratories. For each individual assay, a binary label is assigned to each small molecule indicating whether or not this small molecule activates (or inhibits) the given biological target.

The dataset spans 5120 different biological targets and encompasses 233,786 unique small molecules. Each target has, on average, 94 datapoints, each mapping a small molecule to an active (or not) label. We refer readers to Stanley et al. (2021) for additional information.

**FS-Mol Experimental Setup.** Stanley et al. (2021) offer several few-shot learning baseline methods on this benchmark. We select three of the best: multi-task learning (Caruana, 1997), model-agnostic meta-learning (MAML) (Finn et al., 2017), and prototypical networks (Snell et al., 2017) to evaluate if transforming their feature space to the learned embedding space may convey performance improvements.

This selection of baselines also has the benefit of fulfilling our “Model Agnostic” criterion as the training paradigms for multi-task learning, gradient-based meta-learning, and prototypical networks are highly dissimilar. For instance, multi-task learning builds a molecular representation amenable to all tasks, gradient-based meta-learning learns a representation that can be quickly adapted to a new target after a

minimal number of training steps, and prototypical networks leverage a notion of distance — rather than inner product — in the task embedding space to determine an example’s association with a label.

While each baseline is dissimilar, they all leverage a learned linear transformation to convert the input feature space to the baseline’s own embedding space. We simply replace this “learned” embedding with our pre-trained embedding. While there is a one-time cost to convert the feature space to the pre-trained embedding space, the model’s computational and runtime complexity actually decreases as the model no longer learns an embedding layer, and there are fewer parameters in the model. Also, in accordance with our experimental focus, we do not perform any additional hyperparameter tuning. We simply use the hyperparameters found by Stanley et al. (2021) for their baseline models. We prefix the methods evaluated in FS-Mol with an **EMB-** to indicate this model is trained on molecular representations from the embedding space rather than the default feature space.

**FS-Mol Results.** Table 2 indicates that simulation-based pre-trained embeddings may significantly improve multi-task learning performance on real-world binding prediction. Performance is most improved at smaller support size splits, likely because injecting prior information into deep learning models is most beneficial when there are few examples to learn from on a downstream task. The increase in performance steadily declines as the support size increases, although it ticks up from a support size of 128 to 256. We believe this discrepancy occurs because the number of targets with 256 examples in the test set is much smaller than the number of targets that can support a training set size of 16, 32, 64, or 128. As a result, and as noted by Stanley et al. (2021), the composition of tasks in the 256-support size test set is significantly different from that of the other support sizes.

Next, we examine whether the embeddings — which are trained with multi-task learning — might improve the performance of baselines using very different learning algorithms like Prototypical Networks or MAML. This is a difficult proposition as the inductive biases fundamental to each learning algorithm are highly dissimilar. Surprisingly, our findings indicate that simulation-based pre-trained embeddings consistently improve performance across all support splits in in both MAML (Table 4) and Prototypical Networks (Table 3). One might achieve even larger performance improvements on these baselines by having the training algorithm in simulation mirror the training algorithm on FS-Mol. We leave this exploration to future work.

Taken in aggregate, our experimental findings on FS-Mol suggest that molecular embeddings learned in simulation may improve the performance of popular deep-learning

Table 3. Prototypical Network test  $\Delta$ AUPRC averaged across all targets on FS-Mol. Note both prototypical networks presented in this table use only GNN features as opposed to the model presented in FS-Mol, which uses both GNN and ECFP features.

Support Size	PROTO ( $\uparrow$ )	EMB-PROTO ( $\uparrow$ )	% increase
16	0.189	0.198	$\Delta 5\%$
32	0.227	0.235	$\Delta 4\%$
64	0.259	0.267	$\Delta 3\%$
128	0.293	0.301	$\Delta 3\%$
256	0.267	0.287	$\Delta 7\%$

Table 4. MAML test  $\Delta$ AUPRC averaged across all targets on FS-Mol. Performance of MAML cited from the FS-Mol paper.

Support Size	MAML ( $\uparrow$ )	EMB-MAML ( $\uparrow$ )	% increase
16	0.165	0.169	$\Delta 2\%$
32	0.172	0.178	$\Delta 3\%$
64	0.178	0.188	$\Delta 6\%$
128	0.197	0.208	$\Delta 6\%$
256	0.190	0.197	$\Delta 4\%$

molecular prediction paradigms. While we see the most improvement when the training algorithm in simulation reflects the training algorithm on FS-Mol, our result demonstrate an improvement even when there is a significant difference between these two methods. Our results are all the more striking as we use the default hyperparameters presented in FS-Mol to train each model, and as we make only a single architecture modification, which actually simplifies the model.

**MoleculeNet Description & Setup.** MoleculeNet (Wu et al., 2018) is a collection of datasets spanning many application areas of machine learning for molecular property prediction. As MoleculeNet has been used by many different works, a plethora of experimental configurations have been proposed throughout the literature, each with its own hyperparameter search space, computation budget for running hyperparameter trials, and dataset splitting protocol (i.e., random splitting vs. scaffold splitting). In order to mitigate issues related to comparability, we evaluate the simulation-based learned embeddings within the official MoleculeNet repository<sup>2</sup> using their hyperparameter search size of 16 trials, across the same search space, and with the same Graph Convolutional Network (GCN) model as the officially reported results. The only difference relates to whether the data is represented by atomic features within the default featurization space or the pre-trained molecular embedding space. We divide our findings into MoleculeNet regression datasets as presented in Table 5 and MoleculeNet classification datasets as presented in Table 6.

**MoleculeNet Results.** We begin our analysis with the MoleculeNet datasets that are conceptually similar to the simulation data we use to learn molecular embeddings—namely BACE Regression, BACE Classification, and Tox21,

<sup>2</sup><https://github.com/deepchem/moleculenet>

Table 5. Test RMSE [lower better] on MoleculeNet Regression Datasets. We report the mean and standard deviation across 3 independent runs. GCN results are taken from the official MoleculeNet repository.

	HOPV ( $\downarrow$ )	Delaney ( $\downarrow$ )	BACE Regression ( $\downarrow$ )	Lipo ( $\downarrow$ )	Clearance ( $\downarrow$ )	FreeSolv ( $\downarrow$ )
GCN	$5.43 \pm 2.43$	<b><math>0.89 \pm 0.23</math></b>	$1.65 \pm 0.13$	$0.78 \pm 0.04$	$52.87 \pm 0.30$	<b><math>0.70 \pm 0.05</math></b>
EMB-GCN	<b><math>3.42 \pm 0.11</math></b>	$0.99 \pm 0.04$	<b><math>1.50 \pm 0.02</math></b>	<b><math>0.67 \pm 0.09</math></b>	<b><math>48.14 \pm 1.2</math></b>	$0.71 \pm 0.02$
% change	<b><math>+\Delta 37\%</math></b>	<b><math>-\Delta 11\%</math></b>	<b><math>+\Delta 9\%</math></b>	<b><math>+\Delta 14\%</math></b>	<b><math>+\Delta 9\%</math></b>	<b><math>-\Delta 1\%</math></b>

Table 6. Test AUC ROC on MoleculeNet Classification Datasets. Mean and standard deviation are computed across 3 independent runs. GCN results are taken from the official MoleculeNet repository.

	BACE Classification ( $\uparrow$ )	BBBP ( $\uparrow$ )	ClinTox ( $\uparrow$ )	Tox21 ( $\uparrow$ )
GCN	$0.817 \pm 0.019$	$0.676 \pm 0.019$	$0.907 \pm 0.018$	$0.710 \pm 0.006$
EMB-GCN	<b><math>0.819 \pm 0.012</math></b>	<b><math>0.683 \pm 0.018</math></b>	<b><math>0.917 \pm 0.020</math></b>	<b><math>0.723 \pm 0.006</math></b>
% change	<b><math>\Delta 0\%</math></b>	<b><math>+\Delta 1\%</math></b>	<b><math>+\Delta 1\%</math></b>	<b><math>+\Delta 2\%</math></b>

which measure the interactions of small molecules with target proteins. While Table 6 indicates only minimal improvement for BACE Classification, Table 5 finds that BACE Regression is substantially improved by using simulation-based embeddings. Moreover, Table 6 shows that, for Tox21, learning from the simulation-derived embeddings improves over learning directly from the feature space by 2 standard deviations.

Now we shift our focus to 7 other MoleculeNet datasets that span a diverse set of biological applications, each of which is quite conceptually dissimilar from the small molecule-target interactions evaluated during simulation. Surprisingly, our empirical results indicate the simulation-based embeddings substantially improve the performance of the GCN model on nearly all of these datasets. The exceptions are FreeSolv and Delaney. Both of these measure a molecule’s solubility in water, and these are cases where the 3D conformations adopted by a small molecule binding to a biological target seem almost entirely irrelevant. Even Lipo, which also contains measurements related to a molecule’s solubility, would also somewhat overlap with small molecule-target interactions as the 3D structures formed by hydrophobic or hydrophilic functional groups are causal for both tasks.

A final surprising result relates to the performance improvement on HOPV. Photovoltaic measurements are another case that seems completely dissimilar to molecular-target interactions. However, this dataset is extremely small, composed of 350 small molecules split across train, validation, and test sets. We posit the smoothness of the embedding space — or the natural ordering among molecules imposed by molecular simulation — may be helpful even on a mostly unrelated dataset when training data is significantly constrained.

Together, our experimental findings on MoleculeNet suggest molecular embeddings learned in simulation may improve the performance of deep learning models across a wide variety of downstream molecular predictions tasks. As anticipated, there is likely an association between task similarity and improvement from transforming the feature

space to the learned embedding space. A similar finding is noted by Sun (2022) in evaluating the benefit of pre-training on many supervised molecular datasets, and the concept of “negative transfer” among conceptually dissimilar tasks is well studied in transfer learning literature in the context of other modalities (Zamir et al., 2018; Standley et al., 2020; Achille et al., 2019; Dwivedi & Roig, 2019).

## 6. Conclusion

In this work, we explore harnessing simulation to learn molecular embeddings and find such embeddings may be integrated into existing deep learning molecular paradigms to improve performance. Our analysis shows the molecular representations learned during simulation place molecules with similar interactions across many targets in close proximity to each other in the embedding space. It is likely this molecular embedding — numerically representing molecules based on their interactions with protein targets rather than classical atomic descriptors — is responsible for the improvements we see in real-world molecular prediction performance.

We hope this work encourages others to explore the intersection of molecular simulation and machine learning for molecular property prediction. Our analysis only represents a first step in exploring this space. Future work may investigate the transfer learning dynamics between simulation and real world datasets as well as explore learning molecular representations on other types of simulations — or even across an ensemble of simulators — to develop molecular embeddings suited to a particular task.

## References

- Achille, A., Lam, M., Tewari, R., Ravichandran, A., Maji, S., Fowlkes, C. C., Soatto, S., and Perona, P. Task2vec: Task embedding for meta-learning. In *Proceedings of the IEEE/CVF international conference on computer vision*, pp. 6430–6439, 2019.



- Ahmad, W., Simon, E., Chithrananda, S., Grand, G., and Ramsundar, B. Chemberta-2: Towards chemical foundation models. *arXiv preprint arXiv:2209.01712*, 2022.
- Brohan, A., Brown, N., Carbajal, J., Chebotar, Y., Dabis, J., Finn, C., Gopalakrishnan, K., Hausman, K., Herzog, A., Hsu, J., et al. Rt-1: Robotics transformer for real-world control at scale. *arXiv preprint arXiv:2212.06817*, 2022.
- Caruana, R. Multitask learning. *Machine learning*, 28(1): 41–75, 1997.
- Chen, W., Tripp, A., and Hernández-Lobato, J. M. Meta-learning feature representations for adaptive gaussian processes via implicit differentiation. *arXiv preprint arXiv:2205.02708*, 2022.
- Corso, G., Cavalleri, L., Beaini, D., Liò, P., and Veličković, P. Principal neighbourhood aggregation for graph nets. *Advances in Neural Information Processing Systems*, 33: 13260–13271, 2020.
- Dwivedi, K. and Roig, G. Representation similarity analysis for efficient task taxonomy & transfer learning. In *Proceedings of the IEEE/CVF Conference on Computer Vision and Pattern Recognition*, pp. 12387–12396, 2019.
- Fang, X., Liu, L., Lei, J., He, D., Zhang, S., Zhou, J., Wang, F., Wu, H., and Wang, H. Chemrl-gem: Geometry enhanced molecular representation learning for property prediction. *arXiv preprint arXiv:2106.06130*, 2021.
- Finn, C., Abbeel, P., and Levine, S. Model-agnostic meta-learning for fast adaptation of deep networks. In *International conference on machine learning*, pp. 1126–1135. PMLR, 2017.
- Friesner, R. A., Banks, J. L., Murphy, R. B., Halgren, T. A., Klicic, J. J., Mainz, D. T., Repasky, M. P., Knoll, E. H., Shelley, M., Perry, J. K., et al. Glide: a new approach for rapid, accurate docking and scoring. 1. method and assessment of docking accuracy. *Journal of medicinal chemistry*, 47(7):1739–1749, 2004.
- Gilmer, J., Schoenholz, S. S., Riley, P. F., Vinyals, O., and Dahl, G. E. Neural message passing for quantum chemistry. In *International conference on machine learning*, pp. 1263–1272. PMLR, 2017.
- Hassani, K. and Khasahmadi, A. H. Contrastive multi-view representation learning on graphs. In *International Conference on Machine Learning*, pp. 4116–4126. PMLR, 2020.
- Hu, W., Liu, B., Gomes, J., Zitnik, M., Liang, P., Pande, V., and Leskovec, J. Strategies for pre-training graph neural networks. *arXiv preprint arXiv:1905.12265*, 2019.
- Jiao, R., Han, J., Huang, W., Rong, Y., and Liu, Y. Energy-motivated equivariant pretraining for 3d molecular graphs. *arXiv preprint arXiv:2207.08824*, 2022.
- Kalashnikov, D., Irpan, A., Pastor, P., Ibarz, J., Herzog, A., Jang, E., Quillen, D., Holly, E., Kalakrishnan, M., Vanhoucke, V., et al. Qt-opt: Scalable deep reinforcement learning for vision-based robotic manipulation. *arxiv e-prints*, page. *arXiv preprint arXiv:1806.10293*, 2018.
- Kendall, M. G. *A Course in the Geometry of n Dimensions*. Courier Corporation, 2004.
- Kingma, D. P. and Ba, J. Adam: A method for stochastic optimization. *arXiv preprint arXiv:1412.6980*, 2014.
- Li, S., Zhou, J., Xu, T., Dou, D., and Xiong, H. Geomgcl: Geometric graph contrastive learning for molecular property prediction. In *Proceedings of the AAAI Conference on Artificial Intelligence*, volume 36, pp. 4541–4549, 2022.
- Maziarka, Ł., Danel, T., Mucha, S., Rataj, K., Tabor, J., and Jastrzebski, S. Molecule attention transformer. *arXiv preprint arXiv:2002.08264*, 2020.
- Paszke, A., Gross, S., Massa, F., Lerer, A., Bradbury, J., Chanan, G., Killeen, T., Lin, Z., Gimelshein, N., Antiga, L., et al. Pytorch: An imperative style, high-performance deep learning library. *Advances in neural information processing systems*, 32, 2019.
- Rogers, D. and Hahn, M. Extended-connectivity fingerprints. *Journal of chemical information and modeling*, 50(5):742–754, 2010.
- Rong, Y., Bian, Y., Xu, T., Xie, W., Wei, Y., Huang, W., and Huang, J. Self-supervised graph transformer on large-scale molecular data. *Advances in Neural Information Processing Systems*, 33:12559–12571, 2020.
- Sadeghi, F. and Levine, S. Cad2rl: Real single-image flight without a single real image. *arXiv preprint arXiv:1611.04201*, 2016.
- Schimunek, J., Seidl, P., Friedrich, L., Kuhn, D., Rippmann, F., Hochreiter, S., and Klambauer, G. Context-enriched molecule representations improve few-shot drug discovery, 2022. URL <https://openreview.net/forum?id=kXXPLBEBVGH>.
- Snell, J., Swersky, K., and Zemel, R. Prototypical networks for few-shot learning. *Advances in neural information processing systems*, 30, 2017.
- Standley, T., Zamir, A., Chen, D., Guibas, L., Malik, J., and Savarese, S. Which tasks should be learned together in multi-task learning? In *International Conference on Machine Learning*, pp. 9120–9132. PMLR, 2020.

- Stanley, M., Bronskill, J. F., Maziarz, K., Misztela, H., Lanini, J., Segler, M., Schneider, N., and Brockschmidt, M. Fs-mol: A few-shot learning dataset of molecules. In *Thirty-fifth Conference on Neural Information Processing Systems Datasets and Benchmarks Track (Round 2)*, 2021.
- Sun, R. Does gnn pretraining help molecular representation? *arXiv preprint arXiv:2207.06010*, 2022.
- Tan, J., Zhang, T., Coumans, E., Iscen, A., Bai, Y., Hafner, D., Bohez, S., and Vanhoucke, V. Sim-to-real: Learning agile locomotion for quadruped robots. *arXiv preprint arXiv:1804.10332*, 2018.
- Tobin, J., Fong, R., Ray, A., Schneider, J., Zaremba, W., and Abbeel, P. Domain randomization for transferring deep neural networks from simulation to the real world. In *2017 IEEE/RSJ international conference on intelligent robots and systems (IROS)*, pp. 23–30. IEEE, 2017.
- Wang, L., Wu, Y., Deng, Y., Kim, B., Pierce, L., Krilov, G., Lupyan, D., Robinson, S., Dahlgren, M. K., Greenwood, J., et al. Accurate and reliable prediction of relative ligand binding potency in prospective drug discovery by way of a modern free-energy calculation protocol and force field. *Journal of the American Chemical Society*, 137(7): 2695–2703, 2015.
- Wang, R., Fang, X., Lu, Y., and Wang, S. The pdbind database: Collection of binding affinities for protein-ligand complexes with known three-dimensional structures. *Journal of medicinal chemistry*, 47(12):2977–2980, 2004.
- Wang, Y., Abuduweili, A., Yao, Q., and Dou, D. Property-aware relation networks for few-shot molecular property prediction. *Advances in Neural Information Processing Systems*, 34:17441–17454, 2021.
- Wang, Z., Sun, H., Yao, X., Li, D., Xu, L., Li, Y., Tian, S., and Hou, T. Comprehensive evaluation of ten docking programs on a diverse set of protein-ligand complexes: the prediction accuracy of sampling power and scoring power. *Physical Chemistry Chemical Physics*, 18(18): 12964–12975, 2016.
- Wu, L., Lin, H., Tan, C., Gao, Z., and Li, S. Z. Self-supervised learning on graphs: Contrastive, generative, or predictive. *IEEE Transactions on Knowledge and Data Engineering*, 2021.
- Wu, Z., Ramsundar, B., Feinberg, E. N., Gomes, J., Geniesse, C., Pappu, A. S., Leswing, K., and Pande, V. Moleculenet: a benchmark for molecular machine learning. *Chemical science*, 9(2):513–530, 2018.
- You, Y., Chen, T., Sui, Y., Chen, T., Wang, Z., and Shen, Y. Graph contrastive learning with augmentations. *Advances in Neural Information Processing Systems*, 33: 5812–5823, 2020.
- Zaidi, S., Schaarschmidt, M., Martens, J., Kim, H., Teh, Y. W., Sanchez-Gonzalez, A., Battaglia, P., Pascanu, R., and Godwin, J. Pre-training via denoising for molecular property prediction. *arXiv preprint arXiv:2206.00133*, 2022.
- Zamir, A. R., Sax, A., Shen, W., Guibas, L. J., Malik, J., and Savarese, S. Taskonomy: Disentangling task transfer learning. In *Proceedings of the IEEE conference on computer vision and pattern recognition*, pp. 3712–3722, 2018.
- Zhu, Y., Xu, Y., Yu, F., Liu, Q., Wu, S., and Wang, L. Graph contrastive learning with adaptive augmentation. In *Proceedings of the Web Conference 2021*, pp. 2069–2080, 2021.

---

# Harnessing Simulation for Molecular Embeddings

## (Supplementary Material)

---

### A. Experimental Design

We offer an overview of the architecture and training parameters used to learn molecular embeddings on our simulation data. While this description can be valuable to some readers, we direct those interested in reproducing our findings or building on our framework to access the code directly. We are currently in the process of developing a github repository to host all code used in this work, a service that supports users downloading our generated simulation dataset, as well as a webserver that can be called over gRPC to convert a list of molecules represented as SMILES strings to molecular embeddings produced by our model.

#### A.1. Architecture Details

To learn on the simulation dataset, we follow a design similar to the multi-task architecture described in FS-Mol (Stanley et al., 2021), adapting their code written in Pytorch (Paszke et al., 2019) to train on our simulation dataset. In particular, we use a 10-layer MPNN (Gilmer et al., 2017) augmented with PNA (Corso et al., 2020), and a graph readout composed of an element-wise max pooling operation, weighted sum, and weighted mean to compose a fixed-dimension feature vector from an arbitrary graph representation. We then pass the representation output from the graph readout through a shallow MLP of hidden dimension 512 and finally use a projection layer composed of a  $[512 \times 1]$  linear transformation for each target in our dataset to map the penultimate representation into a predicted regression binding affinity score between the input and the multi-task label. We use a mean squared error loss to train the model.

#### A.2. Training Parameters

Our architecture employs a learning rate of  $5e-5$  for the shared parameters and a learning rate of  $1e-4$  for the task-specific parameters. We use a linear warm-up scheduler for 100 steps (starting at 0 and ending at the specified learning rate) for both shared and task-specific learning rates. The training process also leverages Adam (Kingma & Ba, 2014) with default Pytorch parameters and uses a batch size of 256 molecules.

We randomly split our simulation data into 80% train and

20% validation, and use early stopping with a window size of 10 epoch. Training is run across 100 epochs, and we load the model parameters with the best validation performance to convert the feature space to an embedding space for downstream molecular prediction tasks.

#### A.3. Integrating the Simulation Model into Existing Deep Learning Paradigms

To integrate the embeddings learned during simulation into existing deep learning paradigms, we simply iterate over the training data of a real-world dataset, featurize the molecules, send the featurized molecules through the simulation model, and then extract the final graph representation output from the GNN layers. We then compose a new dataset mapping the molecular embedding to its appropriate label in the original real-world dataset.

Oftentimes, deep learning models fitting molecular prediction tasks will learn a node embedding layer which projects the initial feature space to an embedding space. For models which employ such a projection, we simply remove it from the model. If a model’s internal hidden representation does not match the learned embedding dimension, a single linear transformation can simply be learned to project each node in the molecular embedding to the per-node hidden dimension space of the downstream model.

### B. MoleculeNet Dataset (Dis)Similarity

Expanding on our analysis of the MoleculeNet datasets in section 5, we go into additional detail in the specific ways one dataset may be similar or dissimilar to the small molecule-target interactions evaluated during simulation.

BACE Regression, BACE Classification, and Tox21 measure the interactions of small molecules with different target proteins. These datasets are conceptually similar to our molecular simulation, and the BACE datasets can even be viewed as one of the 5,135 biological targets in FS-Mol. BBBP, ClinTox, and Clearance contain measurements that are related to processes at the organ or organism level and arise from a combination of many factors, including interactions with a host of proteins and membrane permeability. In this way, some parts of the physical generative process are related to the pre-training data, but these measurements

correspond to much higher-level phenomena making it unclear *a priori* if the knowledge gained from pre-training would be relevant. Delaney, FreeSolv, and Lipo measure, roughly speaking, the relative favorability of each molecule occurring in water as compared to in a crystalline form, a vacuum, or a hydrophobic solvent, respectively. Of these, Lipo is the most conceptually similar to small molecule-target docking simulation, as hydrophobic and hydrophilic functional groups are causal for both tasks. HOPV maps small molecules to photovoltaic measurements. While conceptually dissimilar from ligand-target docking simulation, this dataset is extremely small, composed of 350 small molecules split across train, validation, and test sets.

### C. Additional FS-Mol Experimental Results

To offer additional insight into the FS-Mol empirical findings in [section 5](#), we present a per-target breakdown of the first 50 targets in the test set of FS-Mol across support size splits of 16, 32, 64, 128, and 256. [Table 7](#) depicts these results for the Multi-Task Learning baseline, [Table 8](#) depicts these results for the Prototypical Networks baseline using GNN features only (as opposed to the model reported in (Stanley et al., 2021) which uses ECFP as well as GNN features)<sup>3</sup>, and [Table 9](#) depicts these results from the MAML baseline. Highlighted values indicate the highest result for this target at the given support size.

---

<sup>3</sup>We focus our analysis to GNN features in Prototypical networks to isolate the effect of transforming the default GNN feature space to the learned embedding space and avoid non-linear interactions between different input modalities.



# Harnessing Simulation for Molecular Embeddings

Table 7. Multi-Task Results measuring  $\Delta$ AUPRC on the first 50 tasks in the test set of FS-Mol.

TASK-ID	16 (EMB-MT)	32 (EMB-MT)	64 (EMB-MT)	128 (EMB-MT)	256 (EMB-MT)	16 (MT)	32 (MT)	64 (MT)	128 (MT)	256 (MT)
1006005	<b>0.57 <math>\pm</math> 0.05</b>	<b>0.62 <math>\pm</math> 0.04</b>	<b>0.63 <math>\pm</math> 0.05</b>	<b>0.62 <math>\pm</math> 0.05</b>	nan	0.54 $\pm$ 0.03	0.54 $\pm$ 0.03	0.55 $\pm$ 0.03	0.56 $\pm$ 0.06	nan
1066254	<b>0.71 <math>\pm</math> 0.07</b>	<b>0.73 <math>\pm</math> 0.06</b>	<b>0.81 <math>\pm</math> 0.06</b>	0.83 $\pm$ 0.10	nan	0.65 $\pm$ 0.05	0.64 $\pm$ 0.09	0.77 $\pm$ 0.07	<b>0.86 <math>\pm</math> 0.11</b>	nan
1119333	<b>0.69 <math>\pm</math> 0.08</b>	<b>0.73 <math>\pm</math> 0.05</b>	<b>0.78 <math>\pm</math> 0.03</b>	<b>0.82 <math>\pm</math> 0.03</b>	<b>0.85 <math>\pm</math> 0.02</b>	0.69 $\pm$ 0.07	0.72 $\pm$ 0.05	0.76 $\pm$ 0.02	0.79 $\pm$ 0.04	0.84 $\pm$ 0.04
1243967	0.62 $\pm$ 0.08	<b>0.72 <math>\pm</math> 0.09</b>	<b>0.74 <math>\pm</math> 0.05</b>	<b>0.80 <math>\pm</math> 0.05</b>	nan	<b>0.63 <math>\pm</math> 0.07</b>	0.66 $\pm$ 0.05	0.71 $\pm$ 0.04	0.76 $\pm$ 0.05	nan
1243970	<b>0.66 <math>\pm</math> 0.06</b>	<b>0.70 <math>\pm</math> 0.04</b>	<b>0.75 <math>\pm</math> 0.05</b>	<b>0.77 <math>\pm</math> 0.04</b>	nan	0.63 $\pm$ 0.06	0.65 $\pm$ 0.04	0.70 $\pm$ 0.02	0.75 $\pm$ 0.05	nan
1613777	0.52 $\pm$ 0.03	0.53 $\pm$ 0.04	<b>0.55 <math>\pm</math> 0.02</b>	<b>0.57 <math>\pm</math> 0.03</b>	<b>0.59 <math>\pm</math> 0.02</b>	<b>0.52 <math>\pm</math> 0.04</b>	<b>0.53 <math>\pm</math> 0.02</b>	0.54 $\pm$ 0.02	0.57 $\pm$ 0.02	0.59 $\pm$ 0.02
1613800	0.42 $\pm$ 0.02	<b>0.43 <math>\pm</math> 0.03</b>	<b>0.43 <math>\pm</math> 0.02</b>	0.45 $\pm$ 0.02	0.47 $\pm$ 0.02	<b>0.42 <math>\pm</math> 0.03</b>	0.42 $\pm$ 0.01	<b>0.43 <math>\pm</math> 0.03</b>	<b>0.45 <math>\pm</math> 0.02</b>	<b>0.47 <math>\pm</math> 0.01</b>
1613898	0.53 $\pm$ 0.03	0.54 $\pm$ 0.06	0.56 $\pm$ 0.04	0.60 $\pm$ 0.07	nan	<b>0.55 <math>\pm</math> 0.04</b>	<b>0.54 <math>\pm</math> 0.06</b>	<b>0.58 <math>\pm</math> 0.04</b>	<b>0.61 <math>\pm</math> 0.08</b>	nan
1613907	<b>0.62 <math>\pm</math> 0.06</b>	<b>0.62 <math>\pm</math> 0.08</b>	0.63 $\pm$ 0.08	0.66 $\pm$ 0.14	nan	0.60 $\pm$ 0.05	<b>0.62 <math>\pm</math> 0.07</b>	<b>0.67 <math>\pm</math> 0.06</b>	<b>0.70 <math>\pm</math> 0.15</b>	nan
1613926	<b>0.67 <math>\pm</math> 0.07</b>	<b>0.69 <math>\pm</math> 0.06</b>	<b>0.74 <math>\pm</math> 0.06</b>	<b>0.85 <math>\pm</math> 0.14</b>	nan	0.61 $\pm$ 0.04	0.60 $\pm$ 0.06	0.69 $\pm$ 0.06	0.73 $\pm$ 0.19	nan
1613949	<b>0.47 <math>\pm</math> 0.08</b>	<b>0.46 <math>\pm</math> 0.06</b>	<b>0.54 <math>\pm</math> 0.04</b>	<b>0.62 <math>\pm</math> 0.12</b>	nan	0.45 $\pm$ 0.06	0.45 $\pm$ 0.06	0.52 $\pm$ 0.06	0.56 $\pm$ 0.12	nan
1614027	<b>0.54 <math>\pm</math> 0.03</b>	<b>0.56 <math>\pm</math> 0.04</b>	<b>0.60 <math>\pm</math> 0.03</b>	<b>0.66 <math>\pm</math> 0.02</b>	<b>0.69 <math>\pm</math> 0.03</b>	0.53 $\pm$ 0.03	<b>0.56 <math>\pm</math> 0.04</b>	0.59 $\pm$ 0.03	0.63 $\pm$ 0.02	0.66 $\pm$ 0.02
1614153	<b>0.36 <math>\pm</math> 0.01</b>	<b>0.38 <math>\pm</math> 0.03</b>	<b>0.38 <math>\pm</math> 0.03</b>	<b>0.40 <math>\pm</math> 0.02</b>	<b>0.40 <math>\pm</math> 0.02</b>	0.36 $\pm$ 0.02	0.37 $\pm$ 0.03	0.37 $\pm$ 0.02	0.38 $\pm$ 0.03	0.39 $\pm$ 0.01
1614292	<b>0.37 <math>\pm</math> 0.03</b>	<b>0.37 <math>\pm</math> 0.02</b>	<b>0.38 <math>\pm</math> 0.02</b>	<b>0.38 <math>\pm</math> 0.02</b>	<b>0.39 <math>\pm</math> 0.01</b>	0.36 $\pm$ 0.02	0.37 $\pm$ 0.01	0.38 $\pm$ 0.02	0.38 $\pm$ 0.01	0.38 $\pm$ 0.02
1614423	<b>0.66 <math>\pm</math> 0.12</b>	<b>0.68 <math>\pm</math> 0.10</b>	<b>0.72 <math>\pm</math> 0.05</b>	<b>0.77 <math>\pm</math> 0.04</b>	<b>0.82 <math>\pm</math> 0.02</b>	0.52 $\pm$ 0.05	0.54 $\pm$ 0.05	0.59 $\pm$ 0.05	0.67 $\pm$ 0.04	0.74 $\pm$ 0.04
1614433	<b>0.45 <math>\pm</math> 0.04</b>	0.47 $\pm$ 0.06	<b>0.48 <math>\pm</math> 0.04</b>	<b>0.50 <math>\pm</math> 0.02</b>	<b>0.55 <math>\pm</math> 0.04</b>	0.45 $\pm$ 0.04	<b>0.47 <math>\pm</math> 0.05</b>	0.47 $\pm$ 0.04	0.49 $\pm$ 0.03	0.53 $\pm$ 0.04
1614466	<b>0.47 <math>\pm</math> 0.04</b>	<b>0.48 <math>\pm</math> 0.05</b>	<b>0.49 <math>\pm</math> 0.03</b>	<b>0.49 <math>\pm</math> 0.05</b>	<b>0.50 <math>\pm</math> 0.03</b>	0.46 $\pm$ 0.05	0.47 $\pm$ 0.05	0.47 $\pm$ 0.04	0.48 $\pm$ 0.04	0.48 $\pm$ 0.02
1614503	<b>0.47 <math>\pm</math> 0.08</b>	<b>0.48 <math>\pm</math> 0.09</b>	<b>0.52 <math>\pm</math> 0.05</b>	<b>0.73 <math>\pm</math> 0.21</b>	nan	0.44 $\pm$ 0.05	0.44 $\pm$ 0.06	0.48 $\pm$ 0.08	0.66 $\pm$ 0.22	nan
1614508	0.74 $\pm$ 0.10	<b>0.85 <math>\pm</math> 0.02</b>	0.87 $\pm$ 0.02	0.90 $\pm$ 0.04	nan	<b>0.76 <math>\pm</math> 0.07</b>	<b>0.85 <math>\pm</math> 0.04</b>	<b>0.87 <math>\pm</math> 0.03</b>	<b>0.91 <math>\pm</math> 0.05</b>	nan
1614522	<b>0.58 <math>\pm</math> 0.04</b>	<b>0.61 <math>\pm</math> 0.04</b>	<b>0.62 <math>\pm</math> 0.03</b>	<b>0.66 <math>\pm</math> 0.01</b>	<b>0.66 <math>\pm</math> 0.03</b>	0.54 $\pm$ 0.04	0.55 $\pm$ 0.02	0.56 $\pm$ 0.02	0.58 $\pm$ 0.03	0.60 $\pm$ 0.02
1737951	<b>0.64 <math>\pm</math> 0.10</b>	<b>0.67 <math>\pm</math> 0.06</b>	<b>0.79 <math>\pm</math> 0.05</b>	<b>0.85 <math>\pm</math> 0.08</b>	nan	0.55 $\pm$ 0.06	0.60 $\pm$ 0.08	0.63 $\pm$ 0.05	0.72 $\pm$ 0.07	nan
1738079	0.50 $\pm$ 0.02	0.50 $\pm$ 0.04	0.49 $\pm$ 0.03	0.48 $\pm$ 0.03	nan	<b>0.52 <math>\pm</math> 0.04</b>	<b>0.52 <math>\pm</math> 0.04</b>	<b>0.53 <math>\pm</math> 0.03</b>	<b>0.56 <math>\pm</math> 0.05</b>	nan
1738362	0.50 $\pm$ 0.10	0.46 $\pm$ 0.08	0.59 $\pm$ 0.09	0.75 $\pm$ 0.20	nan	<b>0.52 <math>\pm</math> 0.07</b>	<b>0.56 <math>\pm</math> 0.11</b>	<b>0.62 <math>\pm</math> 0.05</b>	<b>0.84 <math>\pm</math> 0.14</b>	nan
1738395	<b>0.51 <math>\pm</math> 0.04</b>	<b>0.49 <math>\pm</math> 0.05</b>	<b>0.50 <math>\pm</math> 0.04</b>	<b>0.54 <math>\pm</math> 0.04</b>	nan	0.49 $\pm$ 0.04	0.48 $\pm$ 0.03	0.50 $\pm$ 0.05	0.51 $\pm$ 0.05	nan
1738485	<b>0.56 <math>\pm</math> 0.02</b>	0.55 $\pm$ 0.03	<b>0.58 <math>\pm</math> 0.06</b>	0.59 $\pm$ 0.04	0.65 $\pm$ 0.06	0.54 $\pm$ 0.04	<b>0.56 <math>\pm</math> 0.03</b>	0.58 $\pm$ 0.04	<b>0.60 <math>\pm</math> 0.06</b>	<b>0.68 <math>\pm</math> 0.06</b>
1738502	<b>0.47 <math>\pm</math> 0.06</b>	<b>0.50 <math>\pm</math> 0.06</b>	<b>0.53 <math>\pm</math> 0.05</b>	<b>0.53 <math>\pm</math> 0.03</b>	<b>0.58 <math>\pm</math> 0.03</b>	0.37 $\pm$ 0.03	0.39 $\pm$ 0.02	0.42 $\pm$ 0.03	0.45 $\pm$ 0.02	0.49 $\pm$ 0.04
1738573	0.51 $\pm$ 0.02	0.52 $\pm$ 0.03	<b>0.54 <math>\pm</math> 0.03</b>	<b>0.55 <math>\pm</math> 0.02</b>	<b>0.57 <math>\pm</math> 0.01</b>	<b>0.52 <math>\pm</math> 0.02</b>	<b>0.53 <math>\pm</math> 0.01</b>	0.53 $\pm$ 0.01	0.54 $\pm$ 0.01	0.56 $\pm$ 0.02
1738579	<b>0.58 <math>\pm</math> 0.05</b>	<b>0.59 <math>\pm</math> 0.05</b>	<b>0.59 <math>\pm</math> 0.04</b>	<b>0.67 <math>\pm</math> 0.04</b>	nan	0.52 $\pm$ 0.03	0.54 $\pm$ 0.04	0.56 $\pm$ 0.03	0.62 $\pm$ 0.04	nan
1738633	<b>0.59 <math>\pm</math> 0.06</b>	<b>0.68 <math>\pm</math> 0.04</b>	<b>0.71 <math>\pm</math> 0.06</b>	0.70 $\pm$ 0.08	nan	0.57 $\pm$ 0.05	0.60 $\pm$ 0.08	0.60 $\pm$ 0.05	<b>0.71 <math>\pm</math> 0.10</b>	nan
1794324	0.52 $\pm$ 0.04	<b>0.54 <math>\pm</math> 0.03</b>	0.55 $\pm$ 0.03	0.57 $\pm$ 0.01	<b>0.60 <math>\pm</math> 0.01</b>	<b>0.53 <math>\pm</math> 0.03</b>	0.54 $\pm$ 0.03	<b>0.56 <math>\pm</math> 0.03</b>	<b>0.58 <math>\pm</math> 0.02</b>	0.60 $\pm$ 0.02
1794504	<b>0.72 <math>\pm</math> 0.06</b>	<b>0.75 <math>\pm</math> 0.05</b>	<b>0.81 <math>\pm</math> 0.04</b>	0.85 $\pm$ 0.24	nan	0.67 $\pm$ 0.04	0.67 $\pm$ 0.06	0.73 $\pm$ 0.05	<b>0.90 <math>\pm</math> 0.21</b>	nan
1794519	0.69 $\pm$ 0.08	<b>0.73 <math>\pm</math> 0.05</b>	0.79 $\pm$ 0.02	<b>0.81 <math>\pm</math> 0.05</b>	nan	<b>0.70 <math>\pm</math> 0.06</b>	0.72 $\pm$ 0.05	<b>0.80 <math>\pm</math> 0.03</b>	0.77 $\pm$ 0.07	nan
1794557	<b>0.52 <math>\pm</math> 0.04</b>	<b>0.53 <math>\pm</math> 0.03</b>	<b>0.56 <math>\pm</math> 0.04</b>	<b>0.58 <math>\pm</math> 0.04</b>	<b>0.60 <math>\pm</math> 0.02</b>	0.51 $\pm$ 0.03	0.53 $\pm$ 0.02	0.53 $\pm$ 0.03	0.53 $\pm$ 0.01	0.54 $\pm$ 0.03
1963701	<b>0.54 <math>\pm</math> 0.03</b>	0.54 $\pm$ 0.02	<b>0.58 <math>\pm</math> 0.04</b>	<b>0.61 <math>\pm</math> 0.04</b>	<b>0.65 <math>\pm</math> 0.03</b>	0.53 $\pm$ 0.03	<b>0.54 <math>\pm</math> 0.04</b>	0.56 $\pm$ 0.03	0.58 $\pm$ 0.03	0.63 $\pm$ 0.03
1963705	<b>0.67 <math>\pm</math> 0.09</b>	<b>0.75 <math>\pm</math> 0.05</b>	<b>0.78 <math>\pm</math> 0.03</b>	<b>0.82 <math>\pm</math> 0.03</b>	<b>0.84 <math>\pm</math> 0.02</b>	0.65 $\pm$ 0.07	0.70 $\pm$ 0.06	0.73 $\pm$ 0.04	0.78 $\pm$ 0.03	0.82 $\pm$ 0.02
1963715	<b>0.61 <math>\pm</math> 0.05</b>	<b>0.59 <math>\pm</math> 0.08</b>	<b>0.68 <math>\pm</math> 0.04</b>	<b>0.72 <math>\pm</math> 0.04</b>	<b>0.75 <math>\pm</math> 0.02</b>	0.50 $\pm$ 0.06	0.50 $\pm$ 0.06	0.56 $\pm$ 0.04	0.60 $\pm$ 0.03	0.65 $\pm$ 0.03
1963721	<b>0.45 <math>\pm</math> 0.08</b>	<b>0.48 <math>\pm</math> 0.08</b>	<b>0.55 <math>\pm</math> 0.06</b>	<b>0.57 <math>\pm</math> 0.07</b>	<b>0.71 <math>\pm</math> 0.09</b>	0.38 $\pm$ 0.05	0.42 $\pm$ 0.04	0.44 $\pm$ 0.03	0.50 $\pm$ 0.05	0.61 $\pm$ 0.08
1963723	<b>0.70 <math>\pm</math> 0.10</b>	<b>0.75 <math>\pm</math> 0.09</b>	<b>0.80 <math>\pm</math> 0.03</b>	<b>0.84 <math>\pm</math> 0.02</b>	<b>0.86 <math>\pm</math> 0.02</b>	0.61 $\pm$ 0.05	0.69 $\pm$ 0.05	0.74 $\pm$ 0.04	0.78 $\pm$ 0.03	0.81 $\pm$ 0.02
1963731	<b>0.74 <math>\pm</math> 0.06</b>	<b>0.79 <math>\pm</math> 0.03</b>	<b>0.82 <math>\pm</math> 0.02</b>	<b>0.87 <math>\pm</math> 0.02</b>	<b>0.89 <math>\pm</math> 0.02</b>	0.63 $\pm$ 0.08	0.70 $\pm$ 0.04	0.75 $\pm$ 0.02	0.79 $\pm$ 0.03	0.82 $\pm$ 0.02
1963741	<b>0.60 <math>\pm</math> 0.05</b>	<b>0.65 <math>\pm</math> 0.05</b>	<b>0.70 <math>\pm</math> 0.04</b>	<b>0.75 <math>\pm</math> 0.03</b>	<b>0.78 <math>\pm</math> 0.02</b>	0.51 $\pm$ 0.08	0.57 $\pm$ 0.06	0.59 $\pm$ 0.05	0.64 $\pm$ 0.04	0.71 $\pm$ 0.03
1963756	<b>0.63 <math>\pm</math> 0.09</b>	<b>0.75 <math>\pm</math> 0.04</b>	<b>0.77 <math>\pm</math> 0.03</b>	<b>0.80 <math>\pm</math> 0.02</b>	<b>0.83 <math>\pm</math> 0.02</b>	0.57 $\pm$ 0.07	0.67 $\pm$ 0.05	0.69 $\pm$ 0.06	0.75 $\pm$ 0.02	0.79 $\pm$ 0.02
1963773	<b>0.59 <math>\pm</math> 0.06</b>	<b>0.61 <math>\pm</math> 0.07</b>	<b>0.65 <math>\pm</math> 0.04</b>	<b>0.69 <math>\pm</math> 0.03</b>	<b>0.72 <math>\pm</math> 0.02</b>	0.54 $\pm$ 0.06	0.57 $\pm$ 0.06	0.61 $\pm$ 0.05	0.65 $\pm$ 0.03	0.70 $\pm$ 0.03
1963799	<b>0.58 <math>\pm</math> 0.07</b>	<b>0.64 <math>\pm</math> 0.04</b>	<b>0.68 <math>\pm</math> 0.04</b>	<b>0.71 <math>\pm</math> 0.03</b>	<b>0.74 <math>\pm</math> 0.04</b>	0.48 $\pm$ 0.06	0.55 $\pm$ 0.05	0.58 $\pm$ 0.07	0.63 $\pm$ 0.05	0.68 $\pm$ 0.07
1963810	<b>0.78 <math>\pm</math> 0.06</b>	<b>0.81 <math>\pm</math> 0.05</b>	<b>0.85 <math>\pm</math> 0.02</b>	<b>0.86 <math>\pm</math> 0.02</b>	<b>0.88 <math>\pm</math> 0.01</b>	0.67 $\pm$ 0.06	0.73 $\pm$ 0.05	0.76 $\pm$ 0.06	0.80 $\pm$ 0.04	0.84 $\pm$ 0.02
1963818	<b>0.71 <math>\pm</math> 0.05</b>	<b>0.74 <math>\pm</math> 0.04</b>	<b>0.78 <math>\pm</math> 0.03</b>	<b>0.80 <math>\pm</math> 0.03</b>	<b>0.82 <math>\pm</math> 0.02</b>	0.66 $\pm$ 0.07	0.68 $\pm$ 0.06	0.72 $\pm$ 0.03	0.76 $\pm$ 0.03	0.79 $\pm$ 0.02
1963819	<b>0.61 <math>\pm</math> 0.07</b>	<b>0.67 <math>\pm</math> 0.06</b>	<b>0.73 <math>\pm</math> 0.06</b>	<b>0.77 <math>\pm</math> 0.05</b>	<b>0.82 <math>\pm</math> 0.01</b>	0.48 $\pm$ 0.05	0.56 $\pm$ 0.07	0.60 $\pm$ 0.08	0.68 $\pm$ 0.06	0.77 $\pm$ 0.02
1963824	<b>0.59 <math>\pm</math> 0.05</b>	<b>0.66 <math>\pm</math> 0.05</b>	<b>0.70 <math>\pm</math> 0.03</b>	<b>0.74 <math>\pm</math> 0.03</b>	<b>0.77 <math>\pm</math> 0.05</b>	0.54 $\pm$ 0.04	0.59 $\pm$ 0.05	0.64 $\pm$ 0.04	0.64 $\pm$ 0.04	0.69 $\pm$ 0.03
1963825	<b>0.62 <math>\pm</math> 0.06</b>	<b>0.69 <math>\pm</math> 0.04</b>	<b>0.70 <math>\pm</math> 0.05</b>	<b>0.75 <math>\pm</math> 0.05</b>	<b>0.81 <math>\pm</math> 0.04</b>	0.57 $\pm$ 0.04	0.61 $\pm$ 0.04	0.64 $\pm$ 0.04	0.65 $\pm$ 0.04	0.69 $\pm$ 0.03
1963827	<b>0.74 <math>\pm</math> 0.09</b>	<b>0.78 <math>\pm</math> 0.06</b>	<b>0.84 <math>\pm</math> 0.03</b>	<b>0.86 <math>\pm</math> 0.01</b>	<b>0.88 <math>\pm</math> 0.02</b>	0.71 $\pm$ 0.06	0.72 $\pm$ 0.08	0.79 $\pm$ 0.05	0.82 $\pm$ 0.02	0.84 $\pm$ 0.02
1963831	<b>0.61 <math>\pm</math> 0.10</b>	<b>0.69 <math>\pm</math> 0.07</b>	<b>0.76 <math>\pm</math> 0.02</b>	<b>0.78 <math>\pm</math> 0.04</b>	<b>0.81 <math>\pm</math> 0.05</b>	0.55 $\pm$ 0.11	0.61 $\pm$ 0.07	0.69 $\pm$ 0.06	0.74 $\pm$ 0.05	0.77 $\pm$ 0.04
1963838	<b>0.56 <math>\pm</math> 0.04</b>	<b>0.57 <math>\pm</math> 0.05</b>	<b>0.59 <math>\pm</math> 0.06</b>	<b>0.67 <math>\pm</math> 0.05</b>	nan	0.54 $\pm$ 0.05	0.55 $\pm$ 0.04	0.58 $\pm$ 0.04	0.62 $\pm$ 0.06	nan

Table 8. Prototypical Results measuring  $\Delta$ AUPRC on the first 50 tasks in the test set of FS-Mol.

TASK-ID	16 (EMB-PROTO)	32 (EMB-PROTO)	64 (EMB-PROTO)	128 (EMB-PROTO)	256 (EMB-PROTO)	16 (PROTO)	32 (PROTO)	64 (PROTO)	128 (PROTO)	256 (PROTO)
1006005	<b>0.61 <math>\pm</math> 0.05</b>	<b>0.63 <math>\pm</math> 0.04</b>	<b>0.66 <math>\pm</math> 0.04</b>	<b>0.69 <math>\pm</math> 0.06</b>	nan	0.56 $\pm$ 0.06	0.61 $\pm$ 0.05	0.65 $\pm$ 0.03	0.66 $\pm$ 0.07	nan
1066254	<b>0.72 <math>\pm</math> 0.07</b>	0.77 $\pm$ 0.06	<b>0.84 <math>\pm</math> 0.04</b>	<b>0.87 <math>\pm</math> 0.10</b>	nan	0.71 $\pm$ 0.08	<b>0.78 <math>\pm</math> 0.06</b>	0.82 $\pm$ 0.06	0.85 $\pm$ 0.08	nan
1119333	<b>0.73 <math>\pm</math> 0.05</b>	<b>0.74 <math>\pm</math> 0.06</b>	<b>0.78 <math>\pm</math> 0.03</b>	<b>0.82 <math>\pm</math> 0.02</b>	<b>0.84 <math>\pm</math> 0.04</b>	0.71 $\pm$ 0.06	0.72 $\pm$ 0.04	<b>0.78 <math>\pm</math> 0.03</b>	0.81 $\pm$ 0.02	0.83 $\pm$ 0.04
1243967	<b>0.78 <math>\pm</math> 0.03</b>	<b>0.81 <math>\pm</math> 0.04</b>	<b>0.83 <math>\pm</math> 0.03</b>	<b>0.84 <math>\pm</math> 0.03</b>	nan	0.73 $\pm$ 0.05	0.76 $\pm$ 0.04	0.80 $\pm$ 0.03	0.81 $\pm$ 0.03	nan
1243970	<b>0.75 <math>\pm</math> 0.05</b>	<b>0.79 <math>\pm</math> 0.04</b>	<b>0.81 <math>\pm</math> 0.03</b>	<b>0.85 <math>\pm</math> 0.03</b>	nan	0.71 $\pm$ 0.07	0.74 $\pm$ 0.04	0.81 $\pm$ 0.03	0.82 $\pm$ 0.05	nan
1613777	0.52 $\pm$ 0.02	<b>0.54 <math>\pm</math> 0.03</b>	0.56 $\pm$ 0.03	0.59 $\pm$ 0.02	0.61 $\pm$ 0.02	<b>0.52 <math>\pm</math> 0.04</b>	0.54 $\pm$ 0.04	<b>0.57 <math>\pm</math> 0.03</b>	<b>0.60 <math>\pm</math> 0.04</b>	<b>0.62 <math>\pm</math> 0.03</b>
1613800	<b>0.42 <math>\pm</math> 0.02</b>	<b>0.44 <math>\pm</math> 0.02</b>	<b>0.46 <math>\pm</math> 0.02</b>	<b>0.48 <math>\pm</math> 0.02</b>	<b>0.50 <math>\pm</math> 0.01</b>	0.41 $\pm$ 0.03	0.43 $\pm$ 0.03	0.45 $\pm$ 0.02	0.46 $\pm$ 0.02	0.48 $\pm$ 0.02
1613898	0.52 $\pm$ 0.02	0.55 $\pm$ 0.04	0.54 $\pm$ 0.04	<b>0.61 <math>\pm</math> 0.07</b>	nan	<b>0.55 <math>\pm</math> 0.04</b>	<b>0.55 <math>\pm</math> 0.05</b>	<b>0.55 <math>\pm</math> 0.03</b>	0.57 $\pm$ 0.08	nan
1613907	<b>0.56 <math>\pm</math> 0.04</b>	0.58 $\pm$ 0.04	0.63 $\pm$ 0.04	0.64 $\pm$ 0.14	nan	0.55 $\pm$ 0.06	<b>0.62 <math>\pm</math> 0.06</b>	<b>0.66 <math>\pm</math> 0.07</b>	<b>0.68 <math>\pm</math> 0.10</b>	nan
1613926	<b>0.70 <math>\pm</math> 0.04</b>	<b>0.74 <math>\pm</math> 0.06</b>	<b>0.77 <math>\pm</math> 0.04</b>	<b>0.88 <math>\pm</math> 0.12</b>	nan	0.65 $\pm$ 0.08	0.70 $\pm$ 0.06	0.76 $\pm$ 0.04	0.86 $\pm$ 0.15	nan
1613949	<b>0.57 <math>\pm</math> 0.08</b>	<b>0.63 <math>\pm</math> 0.05</b>	<b>0.67 <math>\pm</math> 0.06</b>	<b>0.67 <math>\pm</math> 0.10</b>	nan	0.53 $\pm$ 0.05	0.57 $\pm$ 0.04	0.58 $\pm$ 0.05	0.63 $\pm$ 0.10	nan
1614027	0.53 $\pm$ 0.02	<b>0.57 <math>\pm</math> 0.02</b>	0.60 $\pm$ 0.03	0.64 $\pm$ 0.02	<b>0.67 <math>\pm</math> 0.02</b>	<b>0.55 <math>\pm</math> 0.02</b>	0.57 $\pm$ 0.04	<b>0.61 <math>\pm</math> 0.04</b>	<b>0.64 <math>\pm</math> 0.02</b>	0.67 $\pm$ 0.02
1614153	<b>0.35 <math>\pm</math> 0.02</b>	0.37 $\pm$ 0.01	0.36 $\pm$ 0.02	0.39 $\pm$ 0.01	<b>0.41 <math>\pm</math> 0.01</b>	0.34 $\pm$ 0.03	<b>0.37 <math>\pm</math> 0.02</b>	<b>0.37 <math>\pm</math> 0.02</b>	<b>0.39 <math>\pm</math> 0.01</b>	<b>0.41 <math>\pm</math> 0.01</b>
1614292	<b>0.36 <math>\pm</math> 0.02</b>	0.38 $\pm$ 0.03	0.39 $\pm$ 0.02	0.40 $\pm$ 0.02	0.41 $\pm$ 0.02	<b>0.36 <math>\pm</math> 0.02</b>	<b>0.39 <math>\pm</math> 0.02</b>	<b>0.41 <math>\pm</math> 0.02</b>	<b>0.42 <math>\pm</math> 0.03</b>	<b>0.44 <math>\pm</math> 0.02</b>
1614423	<b>0.68 <math>\pm</math> 0.06</b>	<b>0.72 <math>\pm</math> 0.04</b>	<b>0.76 <math>\pm</math> 0.02</b>	<b>0.78 <math>\pm</math> 0.02</b>	<b>0.79 <math>\pm</math> 0.04</b>	0.54 $\pm$ 0.07	0.58 $\pm$ 0.05	0.67 $\pm$ 0.04	0.73 $\pm$ 0.02	0.77 $\pm$ 0.02
1614433	<b>0.49 <math>\pm</math> 0.04</b>	<b>0.50 <math>\pm</math> 0.04</b>	<b>0.51 <math>\pm</math> 0.03</b>	<b>0.53 <math>\pm</math> 0.02</b>	0.54 $\pm$ 0.02	0.46 $\pm$ 0.04	0.48 $\pm$ 0.02	0.48 $\pm$ 0.03	0.52 $\pm$ 0.03	<b>0.54 <math>\pm</math> 0.04</b>
1614466	0.47 $\pm$ 0.03	0.48 $\pm$ 0.04	0.49 $\pm$ 0.01	0.51 $\pm$ 0.03	0.53 $\pm$ 0.03	<b>0.48 <math>\pm</math> 0.05</b>	<b>0.53 <math>\pm</math> 0.05</b>	<b>0.53 <math>\pm</math> 0.04</b>	<b>0.57 <math>\pm</math> 0.02</b>	<b>0.58 <math>\pm</math> 0.01</b>
1614503	<b>0.49 <math>\pm</math> 0.03</b>	0.51 $\pm$ 0.07	0.56 $\pm$ 0.06	0.70 $\pm$ 0.22	nan	0.49 $\pm$ 0.07	<b>0.55 <math>\pm</math> 0.05</b>	<b>0.59 <math>\pm</math> 0.02</b>	<b>0.76 <math>\pm</math> 0.22</b>	nan
1614508	0.84 $\pm$ 0.02	0.85 $\pm$ 0.03	0.86 $\pm$ 0.03	<b>0.89 <math>\pm</math> 0.04</b>	nan	<b>0.86 <math>\pm</math> 0.02</b>	<b>0.86 <math>\pm</math> 0.02</b>	<b>0.87 <math>\pm</math> 0.02</b>	0.88 $\pm$ 0.04	nan
1614522	<b>0.58 <math>\pm</math> 0.04</b>	<b>0.61 <math>\pm</math> 0.03</b>	0.60 $\pm$ 0.03	<b>0.64 <math>\pm</math> 0.02</b>	0.67 $\pm$ 0.03	<b>0.58 <math>\pm</math> 0.03</b>	0.60 $\pm$ 0.03	<b>0.61 <math>\pm</math> 0.03</b>	<b>0.64 <math>\pm</math> 0.02</b>	<b>0.67 <math>\pm</math> 0.02</b>
1737951	<b>0.65 <math>\pm</math> 0.08</b>	<b>0.71 <math>\pm</math> 0.06</b>	<b>0.76 <math>\pm</math> 0.04</b>	<b>0.80 <math>\pm</math> 0.06</b>	nan	0.63 $\pm$ 0.06	0.67 $\pm$ 0.05	0.71 $\pm$ 0.04	0.75 $\pm$ 0.07	nan
1738079	0.49 $\pm$ 0.03	0.49 $\pm$ 0.03	0.50 $\pm$ 0.04	0.49 $\pm$ 0.04	nan	<b>0.49 <math>\pm</math> 0.02</b>	<b>0.49 <math>\pm</math> 0.03</b>	<b>0.50 <math>\pm</math> 0.03</b>	<b>0.54 <math>\pm</math> 0.06</b>	nan
1738362	0.46 $\pm$ 0.06	0.55 $\pm$ 0.08	0.59 $\pm$ 0.06	0.64 $\pm$ 0.22	nan	<b>0.49 <math>\pm</math> 0.10</b>	<b>0.56 <math>\pm</math> 0.09</b>	<b>0.65 <math>\pm</math> 0.05</b>	<b>0.82 <math>\pm</math> 0.17</b>	nan
1738395	0.53 $\pm$ 0.05	0.51 $\pm$ 0.04	0.52 $\pm$ 0.03	0.57 $\pm$ 0.04	nan	<b>0.53 <math>\pm</math> 0.04</b>	<b>0.53 <math>\pm</math> 0.04</b>	<b>0.54 <math>\pm</math> 0.05</b>	<b>0.58 <math>\pm</math> 0.06</b>	nan
1738485	0.54 $\pm$ 0.04	0.57 $\pm$ 0.04	0.58 $\pm$ 0.05	<b>0.63 <math>\pm</math> 0.04</b>	<b>0.69 <math>\pm</math> 0.05</b>	<b>0.58 <math>\pm</math> 0.03</b>	<b>0.59 <math>\pm</math> 0.03</b>	<b>0.61 <math>\pm</math> 0.04</b>	0.62 $\pm$ 0.03	0.64 $\pm$ 0.07
1738502	0.41 $\pm$ 0.07	0.44 $\pm$ 0.05	0.47 $\pm$ 0.04	0.49 $\pm$ 0.03	<b>0.53 <math>\pm</math> 0.03</b>	<b>0.42 <math>\pm</math> 0.07</b>	<b>0.45 <math>\pm</math> 0.05</b>	<b>0.48 <math>\pm</math> 0.03</b>	<b>0.49 <math>\pm</math> 0.02</b>	0.52 $\pm$ 0.02
1738573	0.52 $\pm$ 0.03	<b>0.53 <math>\pm</math> 0.03</b>	<b>0.54 <math>\pm</math> 0.02</b>	<b>0.56 <math>\pm</math> 0.02</b>	<b>0.57 <math>\pm</math> 0.02</b>	<b>0.53 <math>\pm</math> 0.02</b>	0.52 $\pm$ 0.02	0.53 $\pm$ 0.02	0.55 $\pm$ 0.01	0.55 $\pm$ 0.01
1738579	0.52 $\pm$ 0.04	0.55 $\pm$ 0.05	0.58 $\pm$ 0.02	<b>0.65 <math>\pm</math> 0.06</b>	nan	<b>0.55 <math>\pm</math> 0.06</b>	<b>0.59 <math>\pm</math> 0.03</b>	<b>0.59 <math>\pm</math> 0.03</b>	0.64 $\pm$ 0.04	nan
1738633	0.56 $\pm$ 0.04	0.58 $\pm$ 0.04	<b>0.59 <math>\pm</math> 0.05</b>	<b>0.63 <math>\pm</math> 0.08</b>	nan	<b>0.56 <math>\pm</math> 0.05</b>	<b>0.59 <math>\pm</math> 0.05</b>	0.59 $\pm$ 0.04	0.62 $\pm$ 0.13	nan
1794324	0.50 $\pm$ 0.03	0.51 $\pm$ 0.03	0.53 $\pm$ 0.03	0.57 $\pm$ 0.02	0.60 $\pm$ 0.02	<b>0.53 <math>\pm</math> 0.03</b>	<b>0.54 <math>\pm</math> 0.02</b>	<b>0.56 <math>\pm</math> 0.03</b>	<b>0.59 <math>\pm</math> 0.02</b>	<b>0.62 <math>\pm</math> 0.02</b>
1794504	<b>0.70 <math>\pm</math> 0.06</b>	<b>0.72 <math>\pm</math> 0.05</b>	<b>0.80 <math>\pm</math> 0.06</b>	<b>0.95 <math>\pm</math> 0.16</b>	nan	0.59 $\pm$ 0.05	0.64 $\pm$ 0.05	0.72 $\pm$ 0.09	<b>0.95 <math>\pm</math> 0.16</b>	nan
1794519	0.65 $\pm$ 0.08	0.72 $\pm$ 0.06	0.78 $\pm$ 0.04	<b>0.82 <math>\pm</math> 0.05</b>	nan	<b>0.73 <math>\pm</math> 0.06</b>	<b>0.78 <math>\pm</math> 0.03</b>	<b>0.81 <math>\pm</math> 0.02</b>	0.79 $\pm$ 0.04	nan
1794557	<b>0.54 <math>\pm</math> 0.02</b>	<b>0.54 <math>\pm</math> 0.02</b>	<b>0.55 <math>\pm</math> 0.02</b>	<b>0.57 <math>\pm</math> 0.03</b>	<b>0.60 <math>\pm</math> 0.02</b>	0.52 $\pm$ 0.02	0.53 $\pm$ 0.02	0.53 $\pm$ 0.03	0.54 $\pm$ 0.03	0.56 $\pm$ 0.02
1963701	<b>0.58 <math>\pm</math> 0.05</b>	<b>0.59 <math>\pm</math> 0.06</b>	<b>0.62 <math>\pm</math> 0.03</b>	<b>0.67 <math>\pm</math> 0.02</b>	<b>0.69 <math>\pm</math> 0.02</b>	0.56 $\pm$ 0.04	0.58 $\pm$ 0.05	0.60 $\pm$ 0.04	0.62 $\pm$ 0.03	0.66 $\pm$ 0.02
1963705	<b>0.74 <math>\pm</math> 0.06</b>	<b>0.77 <math>\pm</math> 0.04</b>	<b>0.81 <math>\pm</math> 0.02</b>	<b>0.83 <math>\pm</math> 0.01</b>	<b>0.84 <math>\pm</math> 0.01</b>	0.71 $\pm$ 0.05	0.74 $\pm$ 0.03	0.78 $\pm$ 0.03	0.80 $\pm$ 0.02	0.81 $\pm$ 0.02
1963715	<b>0.63 <math>\pm</math> 0.10</b>	<b>0.68 <math>\pm</math> 0.05</b>	<b>0.72 <math>\pm</math> 0.03</b>	<b>0.76 <math>\pm</math> 0.02</b>	<b>0.78 <math>\pm</math> 0.02</b>	0.57 $\pm$ 0.07	0.61 $\pm$ 0.03	0.65 $\pm$ 0.03	0.69 $\pm$ 0.02	0.72 $\pm$ 0.02
1963721	<b>0.47 <math>\pm</math> 0.07</b>	<b>0.52 <math>\pm</math> 0.04</b>	<b>0.54 <math>\pm</math> 0.04</b>	<b>0.58 <math>\pm</math> 0.04</b>	<b>0.63 <math>\pm</math> 0.08</b>	0.45 $\pm$ 0.06	0.47 $\pm$ 0.04	0.51 $\pm$ 0.04	0.53 $\pm$ 0.03	0.61 $\pm$ 0.10
1963723	<b>0.77 <math>\pm</math> 0.05</b>	<b>0.80 <math>\pm</math> 0.04</b>	<b>0.84 <math>\pm</math> 0.01</b>	<b>0.86 <math>\pm</math> 0.01</b>	<b>0.87 <math>\pm</math> 0.01</b>	0.72 $\pm$ 0.08	0.79 $\pm$ 0.03	0.81 $\pm$ 0.01	0.83 $\pm$ 0.01	0.85 $\pm$ 0.01
1963731	0.79 $\pm$ 0.06	<b>0.84 <math>\pm</math> 0.02</b>	<b>0.87 <math>\pm</math> 0.02</b>	<b>0.89 <math>\pm</math> 0.01</b>	<b>0.90 <math>\pm</math> 0.01</b>	<b>0.80 <math>\pm</math> 0.05</b>	0.83 $\pm$ 0.02	0.86 $\pm$ 0.01	0.87 $\pm$ 0.01	0.88 $\pm$ 0.01
1963741	<b>0.64 <math>\pm</math> 0.06</b>	<b>0.70 <math>\pm</math> 0.04</b>	<b>0.74 <math>\pm</math> 0.02</b>	<b>0.76 <math>\pm</math> 0.02</b>	<b>0.78 <math>\pm</math> 0.02</b>	0.59 $\pm$ 0.03	0.63 $\pm$ 0.04	0.68 $\pm$ 0.04	0.71 $\pm$ 0.02	0.73 $\pm$ 0.02
1963756	<b>0.74 <math>\pm</math> 0.06</b>	<b>0.77 <math>\pm</math> 0.03</b>	<b>0.79 <math>\pm</math> 0.02</b>	<b>0.82 <math>\pm</math> 0.01</b>	<b>0.84 <math>\pm</math> 0.01</b>	0.63 $\pm$ 0.06	0.68 $\pm$ 0.04	0.73 $\pm$ 0.02	0.76 $\pm$ 0.02	0.77 $\pm$ 0.03
1963773	<b>0.62 <math>\pm</math> 0.09</b>	0.64 $\pm$ 0.06	<b>0.69 <math>\pm</math> 0.04</b>	0.72 $\pm$ 0.03	<b>0.75 <math>\pm</math> 0.01</b>	0.61 $\pm$ 0.07	<b>0.65 <math>\pm</math> 0.06</b>	0.69 $\pm$ 0.04	<b>0.73 <math>\pm</math> 0.02</b>	0.74 $\pm$ 0.03
1963799	<b>0.65 <math>\pm</math> 0.07</b>	<b>0.67 <math>\pm</math> 0.05</b>	<b>0.69 <math>\pm</math> 0.02</b>	<b>0.74 <math>\pm</math> 0.02</b>	<b>0.76 <math>\pm</math> 0.03</b>	0.56 $\pm$ 0.07	0.63 $\pm$ 0.04	0.67 $\pm$ 0.03	0.69 $\pm$ 0.02	0.72 $\pm$ 0.05
1963810	<b>0.80 <math>\pm</math> 0.04</b>	<b>0.83 <math>\pm</math> 0.03</b>	<b>0.86 <math>\pm</math> 0.01</b>	<b>0.86 <math>\pm</math> 0.01</b>	<b>0.88 <math>\pm</math> 0.01</b>	0.76 $\pm$ 0.06	0.79 $\pm$ 0.04	0.82 $\pm$ 0.02	0.85 $\pm$ 0.01	0.87 $\pm$ 0.01
1963818	<b>0.71 <math>\pm</math> 0.06</b>	0.75 $\pm$ 0.05	0.78 $\pm$ 0.03	<b>0.82 <math>\pm</math> 0.02</b>	<b>0.84 <math>\pm</math> 0.02</b>	<b>0.71 <math>\pm</math> 0.03</b>	0.73 $\pm$ 0.04	<b>0.78 <math>\pm</math> 0.02</b>	0.81 $\pm$ 0.01	0.82 $\pm$ 0.01
1963819	<b>0.65 <math>\pm</math> 0.08</b>	0.68 $\pm$ 0.06	<b>0.74 <math>\pm</math> 0.03</b>	0.78 $\pm$ 0.03	0.81 $\pm$ 0.02	0.62 $\pm$ 0.12	<b>0.70 <math>\pm</math> 0.05</b>	0.73 $\pm$ 0.05	<b>0.79 <math>\pm</math> 0.02</b>	<b>0.81 <math>\pm</math> 0.02</b>
1963824	<b>0.60 <math>\pm</math> 0.06</b>	<b>0.63 <math>\pm</math> 0.04</b>	<b>0.67 <math>\pm</math> 0.05</b>	<b>0.72 <math>\pm</math> 0.04</b>	<b>0.75 <math>\pm</math> 0.03</b>	0.52 $\pm$ 0.04	0.54 $\pm$ 0.03	0.57 $\pm$ 0.03	0.61 $\pm$ 0.03	0.62 $\pm$ 0.06
1963825	<b>0.66 <math>\pm</math> 0.06</b>	<b>0.70 <math>\pm</math> 0.05</b>	<b>0.72 <math>\pm</math> 0.03</b>	<b>0.74 <math>\pm</math> 0.02</b>	<b>0.78 <math>\pm</math> 0.04</b>	0.62 $\pm$ 0.07	0.68 $\pm$ 0.03	0.71 $\pm$ 0.04	0.73 $\pm$ 0.02	0.77 $\pm$ 0.03
1963827	<b>0.78 <math>\pm</math> 0.06</b>	<b>0.81 <math>\pm</math> 0.03</b>	<b>0.86 <math>\pm</math> 0.02</b>	<b>0.88 <math>\pm</math> 0.00</b>	<b>0.88 <math>\pm</math> 0.01</b>	0.77 $\pm$ 0.04	0.80 $\pm$ 0.04	0.84 $\pm$ 0.02	0.86 $\pm$ 0.01	0.87 $\pm$ 0.01
1963831	<b>0.62 <math>\pm</math> 0.10</b>	0.69 $\pm$ 0.07	0.74 $\pm$ 0.03	0.77 $\pm$ 0.03	0.78 $\pm$ 0.05	0.61 $\pm$ 0.08	<b>0.69 <math>\pm</math> 0.05</b>	<b>0.76 <math>\pm</math> 0.03</b>	<b>0.78 <math>\pm</math> 0.02</b>	<b>0.79 <math>\pm</math> 0.06</b>
1963838	0.52 $\pm$ 0.03	0.55 $\pm$ 0.02	0.58 $\pm$ 0.03	0.60 $\pm$ 0.03	nan	<b>0.55 <math>\pm</math> 0.03</b>	<b>0.57 <math>\pm</math> 0.05</b>	<b>0.61 <math>\pm</math> 0.04</b>	<b>0.64 <math>\pm</math> 0.03</b>	nan

# Harnessing Simulation for Molecular Embeddings

Table 9. MAML results measuring  $\Delta$ AUPRC on the first 50 tasks in the test set of FS-Mol.

TASK-ID	16 (EMB-MAML)	32 (EMB-MAML)	64 (EMB-MAML)	128 (EMB-MAML)	256 (EMB-MAML)	16 (MAML)	32 (MAML)	64 (MAML)	128 (MAML)	256 (MAML)
1006005	0.47 $\pm$ 0.03	0.49 $\pm$ 0.05	0.49 $\pm$ 0.04	0.54 $\pm$ 0.06	nan	<b>0.49 <math>\pm</math> 0.02</b>	<b>0.51 <math>\pm</math> 0.04</b>	<b>0.52 <math>\pm</math> 0.03</b>	<b>0.56 <math>\pm</math> 0.05</b>	nan
1066254	<b>0.58 <math>\pm</math> 0.07</b>	<b>0.61 <math>\pm</math> 0.05</b>	<b>0.65 <math>\pm</math> 0.07</b>	<b>0.65 <math>\pm</math> 0.13</b>	nan	0.56 $\pm$ 0.07	0.58 $\pm$ 0.04	0.59 $\pm$ 0.07	0.63 $\pm$ 0.15	nan
1119333	<b>0.73 <math>\pm</math> 0.03</b>	<b>0.74 <math>\pm</math> 0.03</b>	<b>0.77 <math>\pm</math> 0.04</b>	<b>0.76 <math>\pm</math> 0.05</b>	<b>0.77 <math>\pm</math> 0.06</b>	0.70 $\pm$ 0.03	0.72 $\pm$ 0.04	0.74 $\pm$ 0.05	0.72 $\pm$ 0.02	0.74 $\pm$ 0.05
1243967	0.72 $\pm$ 0.03	<b>0.76 <math>\pm</math> 0.03</b>	<b>0.75 <math>\pm</math> 0.04</b>	<b>0.77 <math>\pm</math> 0.04</b>	nan	<b>0.72 <math>\pm</math> 0.05</b>	0.75 $\pm$ 0.01	0.74 $\pm$ 0.04	0.76 $\pm$ 0.04	nan
1243970	0.70 $\pm$ 0.04	0.71 $\pm$ 0.01	0.70 $\pm$ 0.02	<b>0.71 <math>\pm</math> 0.03</b>	nan	<b>0.71 <math>\pm</math> 0.03</b>	<b>0.72 <math>\pm</math> 0.03</b>	<b>0.72 <math>\pm</math> 0.03</b>	0.68 $\pm$ 0.03	nan
1613777	<b>0.53 <math>\pm</math> 0.01</b>	<b>0.53 <math>\pm</math> 0.01</b>	<b>0.53 <math>\pm</math> 0.01</b>	<b>0.54 <math>\pm</math> 0.02</b>	<b>0.54 <math>\pm</math> 0.02</b>	0.50 $\pm$ 0.01	0.51 $\pm$ 0.01	0.51 $\pm$ 0.01	0.53 $\pm$ 0.02	0.53 $\pm$ 0.02
1613800	<b>0.40 <math>\pm</math> 0.00</b>	<b>0.40 <math>\pm</math> 0.01</b>	<b>0.41 <math>\pm</math> 0.01</b>	<b>0.42 <math>\pm</math> 0.01</b>	<b>0.42 <math>\pm</math> 0.01</b>	<b>0.40 <math>\pm</math> 0.01</b>	0.40 $\pm$ 0.01	0.40 $\pm$ 0.01	0.41 $\pm$ 0.01	0.41 $\pm$ 0.01
1613898	0.56 $\pm$ 0.02	0.55 $\pm$ 0.04	<b>0.58 <math>\pm</math> 0.04</b>	<b>0.57 <math>\pm</math> 0.08</b>	nan	<b>0.57 <math>\pm</math> 0.02</b>	<b>0.56 <math>\pm</math> 0.03</b>	0.56 $\pm$ 0.03	0.56 $\pm$ 0.04	nan
1613907	<b>0.54 <math>\pm</math> 0.03</b>	<b>0.55 <math>\pm</math> 0.04</b>	<b>0.54 <math>\pm</math> 0.06</b>	<b>0.55 <math>\pm</math> 0.07</b>	nan	0.53 $\pm$ 0.03	0.51 $\pm$ 0.02	0.53 $\pm$ 0.05	0.55 $\pm$ 0.13	nan
1613926	<b>0.67 <math>\pm</math> 0.04</b>	<b>0.65 <math>\pm</math> 0.06</b>	<b>0.71 <math>\pm</math> 0.06</b>	<b>0.78 <math>\pm</math> 0.20</b>	nan	0.57 $\pm$ 0.09	0.59 $\pm$ 0.10	0.65 $\pm$ 0.12	0.77 $\pm$ 0.12	nan
1613949	0.46 $\pm$ 0.04	0.47 $\pm$ 0.04	0.47 $\pm$ 0.05	<b>0.45 <math>\pm</math> 0.10</b>	nan	<b>0.48 <math>\pm</math> 0.03</b>	<b>0.48 <math>\pm</math> 0.04</b>	<b>0.48 <math>\pm</math> 0.06</b>	0.43 $\pm$ 0.09	nan
1614027	0.51 $\pm$ 0.02	0.52 $\pm$ 0.02	<b>0.54 <math>\pm</math> 0.02</b>	<b>0.57 <math>\pm</math> 0.03</b>	<b>0.60 <math>\pm</math> 0.02</b>	<b>0.52 <math>\pm</math> 0.01</b>	<b>0.52 <math>\pm</math> 0.01</b>	0.53 $\pm$ 0.03	0.54 $\pm$ 0.03	0.58 $\pm$ 0.04
1614153	0.33 $\pm$ 0.01	0.34 $\pm$ 0.01	0.33 $\pm$ 0.01	0.34 $\pm$ 0.01	0.34 $\pm$ 0.01	<b>0.33 <math>\pm</math> 0.01</b>	<b>0.34 <math>\pm</math> 0.01</b>	<b>0.34 <math>\pm</math> 0.01</b>	<b>0.35 <math>\pm</math> 0.01</b>	<b>0.36 <math>\pm</math> 0.01</b>
1614292	<b>0.35 <math>\pm</math> 0.02</b>	<b>0.36 <math>\pm</math> 0.02</b>	<b>0.37 <math>\pm</math> 0.02</b>	<b>0.37 <math>\pm</math> 0.02</b>	<b>0.39 <math>\pm</math> 0.01</b>	0.35 $\pm$ 0.01	0.35 $\pm$ 0.01	0.35 $\pm$ 0.01	0.35 $\pm$ 0.01	0.35 $\pm$ 0.01
1614423	0.44 $\pm$ 0.07	<b>0.52 <math>\pm</math> 0.10</b>	<b>0.64 <math>\pm</math> 0.03</b>	<b>0.69 <math>\pm</math> 0.05</b>	<b>0.71 <math>\pm</math> 0.04</b>	<b>0.45 <math>\pm</math> 0.05</b>	0.47 $\pm$ 0.07	0.51 $\pm$ 0.07	0.60 $\pm$ 0.07	0.68 $\pm$ 0.02
1614433	<b>0.46 <math>\pm</math> 0.02</b>	0.46 $\pm$ 0.02	<b>0.47 <math>\pm</math> 0.02</b>	<b>0.49 <math>\pm</math> 0.03</b>	<b>0.52 <math>\pm</math> 0.04</b>	0.44 $\pm$ 0.01	<b>0.46 <math>\pm</math> 0.03</b>	0.47 $\pm$ 0.03	0.48 $\pm$ 0.04	0.49 $\pm$ 0.04
1614466	0.46 $\pm$ 0.01	0.46 $\pm$ 0.02	0.47 $\pm$ 0.02	0.47 $\pm$ 0.02	0.51 $\pm$ 0.03	<b>0.47 <math>\pm</math> 0.01</b>	<b>0.48 <math>\pm</math> 0.02</b>	<b>0.49 <math>\pm</math> 0.02</b>	<b>0.49 <math>\pm</math> 0.02</b>	<b>0.51 <math>\pm</math> 0.03</b>
1614503	0.35 $\pm$ 0.04	<b>0.36 <math>\pm</math> 0.06</b>	0.37 $\pm$ 0.04	0.56 $\pm$ 0.24	nan	<b>0.37 <math>\pm</math> 0.02</b>	0.36 $\pm$ 0.03	<b>0.38 <math>\pm</math> 0.04</b>	<b>0.57 <math>\pm</math> 0.20</b>	nan
1614508	<b>0.70 <math>\pm</math> 0.12</b>	0.77 $\pm$ 0.13	<b>0.80 <math>\pm</math> 0.05</b>	0.82 $\pm$ 0.09	nan	0.66 $\pm$ 0.08	<b>0.79 <math>\pm</math> 0.07</b>	0.77 $\pm$ 0.09	<b>0.83 <math>\pm</math> 0.09</b>	nan
1614522	<b>0.52 <math>\pm</math> 0.05</b>	<b>0.53 <math>\pm</math> 0.03</b>	<b>0.54 <math>\pm</math> 0.06</b>	<b>0.61 <math>\pm</math> 0.02</b>	<b>0.62 <math>\pm</math> 0.02</b>	0.50 $\pm$ 0.03	0.52 $\pm$ 0.02	0.52 $\pm$ 0.04	0.56 $\pm$ 0.03	0.58 $\pm$ 0.03
1737951	0.49 $\pm$ 0.09	0.46 $\pm$ 0.07	<b>0.61 <math>\pm</math> 0.03</b>	<b>0.67 <math>\pm</math> 0.06</b>	nan	<b>0.57 <math>\pm</math> 0.04</b>	<b>0.57 <math>\pm</math> 0.03</b>	0.58 $\pm$ 0.04	0.58 $\pm$ 0.07	nan
1738079	0.48 $\pm$ 0.01	0.47 $\pm$ 0.01	0.47 $\pm$ 0.02	0.49 $\pm$ 0.04	nan	<b>0.52 <math>\pm</math> 0.01</b>	<b>0.51 <math>\pm</math> 0.01</b>	<b>0.51 <math>\pm</math> 0.03</b>	<b>0.52 <math>\pm</math> 0.03</b>	nan
1738362	0.31 $\pm$ 0.03	0.34 $\pm$ 0.05	0.34 $\pm$ 0.07	<b>0.64 <math>\pm</math> 0.23</b>	nan	<b>0.37 <math>\pm</math> 0.01</b>	<b>0.38 <math>\pm</math> 0.03</b>	<b>0.40 <math>\pm</math> 0.04</b>	0.46 $\pm$ 0.19	nan
1738395	0.49 $\pm$ 0.03	<b>0.50 <math>\pm</math> 0.03</b>	<b>0.49 <math>\pm</math> 0.03</b>	0.50 $\pm$ 0.05	nan	<b>0.50 <math>\pm</math> 0.03</b>	0.48 $\pm$ 0.03	0.48 $\pm$ 0.03	<b>0.50 <math>\pm</math> 0.05</b>	nan
1738485	<b>0.49 <math>\pm</math> 0.01</b>	<b>0.51 <math>\pm</math> 0.02</b>	<b>0.52 <math>\pm</math> 0.04</b>	<b>0.54 <math>\pm</math> 0.04</b>	<b>0.55 <math>\pm</math> 0.06</b>	0.49 $\pm$ 0.01	0.49 $\pm$ 0.01	0.48 $\pm$ 0.01	0.50 $\pm$ 0.06	0.54 $\pm$ 0.06
1738502	0.39 $\pm$ 0.01	0.40 $\pm$ 0.02	0.40 $\pm$ 0.02	<b>0.43 <math>\pm</math> 0.04</b>	<b>0.43 <math>\pm</math> 0.04</b>	<b>0.41 <math>\pm</math> 0.01</b>	<b>0.42 <math>\pm</math> 0.02</b>	<b>0.41 <math>\pm</math> 0.02</b>	0.41 $\pm$ 0.02	0.41 $\pm$ 0.02
1738573	0.51 $\pm$ 0.02	0.50 $\pm$ 0.01	0.51 $\pm$ 0.02	<b>0.52 <math>\pm</math> 0.02</b>	<b>0.53 <math>\pm</math> 0.02</b>	<b>0.52 <math>\pm</math> 0.01</b>	<b>0.51 <math>\pm</math> 0.01</b>	<b>0.52 <math>\pm</math> 0.01</b>	0.52 $\pm$ 0.01	0.52 $\pm$ 0.01
1738579	<b>0.54 <math>\pm</math> 0.03</b>	<b>0.56 <math>\pm</math> 0.02</b>	<b>0.56 <math>\pm</math> 0.03</b>	<b>0.60 <math>\pm</math> 0.05</b>	nan	0.53 $\pm$ 0.03	0.55 $\pm$ 0.03	0.55 $\pm$ 0.04	0.58 $\pm$ 0.04	nan
1738633	0.55 $\pm$ 0.04	0.56 $\pm$ 0.04	0.60 $\pm$ 0.04	0.57 $\pm$ 0.09	nan	<b>0.59 <math>\pm</math> 0.02</b>	<b>0.60 <math>\pm</math> 0.02</b>	<b>0.60 <math>\pm</math> 0.04</b>	<b>0.63 <math>\pm</math> 0.12</b>	nan
1794324	<b>0.52 <math>\pm</math> 0.02</b>	<b>0.52 <math>\pm</math> 0.01</b>	<b>0.52 <math>\pm</math> 0.01</b>	<b>0.53 <math>\pm</math> 0.02</b>	<b>0.54 <math>\pm</math> 0.02</b>	0.51 $\pm$ 0.00	0.51 $\pm$ 0.01	0.52 $\pm$ 0.01	0.52 $\pm$ 0.01	0.53 $\pm$ 0.01
1794504	<b>0.68 <math>\pm</math> 0.01</b>	<b>0.70 <math>\pm</math> 0.04</b>	<b>0.71 <math>\pm</math> 0.04</b>	<b>0.85 <math>\pm</math> 0.24</b>	nan	0.65 $\pm$ 0.05	0.66 $\pm$ 0.05	0.71 $\pm$ 0.04	<b>0.85 <math>\pm</math> 0.24</b>	nan
1794519	0.64 $\pm$ 0.05	<b>0.66 <math>\pm</math> 0.07</b>	<b>0.69 <math>\pm</math> 0.08</b>	<b>0.73 <math>\pm</math> 0.13</b>	nan	<b>0.64 <math>\pm</math> 0.07</b>	0.62 $\pm$ 0.05	0.65 $\pm$ 0.07	0.71 $\pm$ 0.11	nan
1794557	0.53 $\pm$ 0.02	0.54 $\pm$ 0.01	0.54 $\pm$ 0.02	0.53 $\pm$ 0.02	0.53 $\pm$ 0.01	<b>0.55 <math>\pm</math> 0.01</b>	<b>0.55 <math>\pm</math> 0.01</b>	<b>0.55 <math>\pm</math> 0.01</b>	<b>0.55 <math>\pm</math> 0.01</b>	<b>0.55 <math>\pm</math> 0.01</b>
1963701	<b>0.60 <math>\pm</math> 0.01</b>	<b>0.59 <math>\pm</math> 0.02</b>	<b>0.59 <math>\pm</math> 0.02</b>	<b>0.60 <math>\pm</math> 0.01</b>	<b>0.60 <math>\pm</math> 0.02</b>	0.60 $\pm$ 0.01	0.59 $\pm$ 0.01	<b>0.59 <math>\pm</math> 0.01</b>	0.59 $\pm$ 0.01	0.59 $\pm$ 0.02
1963705	0.71 $\pm$ 0.03	0.70 $\pm$ 0.02	0.72 $\pm$ 0.01	0.72 $\pm$ 0.01	0.71 $\pm$ 0.02	<b>0.77 <math>\pm</math> 0.01</b>	<b>0.77 <math>\pm</math> 0.02</b>	<b>0.77 <math>\pm</math> 0.01</b>	<b>0.77 <math>\pm</math> 0.03</b>	<b>0.76 <math>\pm</math> 0.04</b>
1963715	<b>0.63 <math>\pm</math> 0.00</b>	<b>0.62 <math>\pm</math> 0.03</b>	0.63 $\pm$ 0.01	0.64 $\pm$ 0.01	0.64 $\pm$ 0.02	0.63 $\pm$ 0.01	0.61 $\pm$ 0.04	<b>0.64 <math>\pm</math> 0.01</b>	<b>0.64 <math>\pm</math> 0.01</b>	<b>0.64 <math>\pm</math> 0.02</b>
1963721	0.50 $\pm$ 0.02	0.50 $\pm$ 0.02	0.50 $\pm$ 0.02	<b>0.51 <math>\pm</math> 0.04</b>	<b>0.55 <math>\pm</math> 0.07</b>	<b>0.52 <math>\pm</math> 0.02</b>	<b>0.51 <math>\pm</math> 0.01</b>	<b>0.52 <math>\pm</math> 0.01</b>	0.51 $\pm$ 0.03	0.54 $\pm$ 0.09
1963723	0.72 $\pm$ 0.03	0.73 $\pm$ 0.01	0.73 $\pm$ 0.01	0.74 $\pm$ 0.02	0.75 $\pm$ 0.02	<b>0.72 <math>\pm</math> 0.03</b>	<b>0.74 <math>\pm</math> 0.02</b>	<b>0.74 <math>\pm</math> 0.01</b>	<b>0.75 <math>\pm</math> 0.02</b>	<b>0.77 <math>\pm</math> 0.02</b>
1963731	0.70 $\pm$ 0.02	0.70 $\pm$ 0.01	0.70 $\pm$ 0.02	0.76 $\pm$ 0.06	0.76 $\pm$ 0.05	<b>0.71 <math>\pm</math> 0.03</b>	<b>0.74 <math>\pm</math> 0.02</b>	<b>0.74 <math>\pm</math> 0.02</b>	<b>0.76 <math>\pm</math> 0.02</b>	<b>0.79 <math>\pm</math> 0.03</b>
1963741	<b>0.65 <math>\pm</math> 0.02</b>	<b>0.66 <math>\pm</math> 0.00</b>	<b>0.66 <math>\pm</math> 0.01</b>	<b>0.67 <math>\pm</math> 0.01</b>	<b>0.67 <math>\pm</math> 0.01</b>	0.65 $\pm$ 0.01	0.65 $\pm$ 0.01	0.66 $\pm$ 0.01	0.65 $\pm$ 0.01	0.65 $\pm$ 0.01
1963756	<b>0.76 <math>\pm</math> 0.05</b>	<b>0.75 <math>\pm</math> 0.04</b>	<b>0.76 <math>\pm</math> 0.04</b>	<b>0.77 <math>\pm</math> 0.02</b>	<b>0.77 <math>\pm</math> 0.01</b>	0.71 $\pm$ 0.02	0.72 $\pm$ 0.03	0.70 $\pm$ 0.04	0.72 $\pm$ 0.02	0.72 $\pm$ 0.03
1963773	0.60 $\pm$ 0.01	0.59 $\pm$ 0.04	0.60 $\pm$ 0.03	0.60 $\pm$ 0.02	0.60 $\pm$ 0.02	<b>0.62 <math>\pm</math> 0.02</b>	<b>0.63 <math>\pm</math> 0.02</b>	<b>0.63 <math>\pm</math> 0.02</b>	<b>0.64 <math>\pm</math> 0.03</b>	<b>0.63 <math>\pm</math> 0.02</b>
1963799	0.63 $\pm$ 0.01	0.62 $\pm$ 0.01	0.61 $\pm$ 0.03	0.61 $\pm$ 0.02	0.60 $\pm$ 0.05	<b>0.64 <math>\pm</math> 0.02</b>	<b>0.66 <math>\pm</math> 0.01</b>	<b>0.66 <math>\pm</math> 0.02</b>	<b>0.67 <math>\pm</math> 0.03</b>	<b>0.67 <math>\pm</math> 0.07</b>
1963810	<b>0.78 <math>\pm</math> 0.01</b>	<b>0.77 <math>\pm</math> 0.02</b>	<b>0.78 <math>\pm</math> 0.01</b>	<b>0.78 <math>\pm</math> 0.01</b>	<b>0.78 <math>\pm</math> 0.01</b>	0.77 $\pm$ 0.01	0.75 $\pm$ 0.03	0.76 $\pm$ 0.02	0.76 $\pm$ 0.02	0.78 $\pm$ 0.02
1963818	<b>0.71 <math>\pm</math> 0.02</b>	<b>0.72 <math>\pm</math> 0.01</b>	0.72 $\pm$ 0.03	<b>0.73 <math>\pm</math> 0.02</b>	<b>0.73 <math>\pm</math> 0.03</b>	0.70 $\pm$ 0.04	0.72 $\pm$ 0.01	<b>0.72 <math>\pm</math> 0.03</b>	0.72 $\pm$ 0.03	0.73 $\pm$ 0.03
1963819	0.59 $\pm$ 0.04	0.61 $\pm$ 0.03	0.59 $\pm$ 0.01	0.61 $\pm$ 0.03	0.61 $\pm$ 0.03	<b>0.60 <math>\pm</math> 0.02</b>	<b>0.61 <math>\pm</math> 0.03</b>	<b>0.62 <math>\pm</math> 0.03</b>	<b>0.63 <math>\pm</math> 0.04</b>	<b>0.63 <math>\pm</math> 0.03</b>
1963824	<b>0.62 <math>\pm</math> 0.04</b>	0.63 $\pm$ 0.02	<b>0.65 <math>\pm</math> 0.04</b>	<b>0.65 <math>\pm</math> 0.04</b>	<b>0.69 <math>\pm</math> 0.05</b>	0.62 $\pm$ 0.03	<b>0.64 <math>\pm</math> 0.04</b>	0.64 $\pm$ 0.04	0.63 $\pm$ 0.03	0.63 $\pm$ 0.04
1963825	0.73 $\pm$ 0.01	0.72 $\pm$ 0.02	0.73 $\pm$ 0.01	0.74 $\pm$ 0.02	0.75 $\pm$ 0.04	<b>0.77 <math>\pm</math> 0.02</b>	<b>0.77 <math>\pm</math> 0.02</b>	<b>0.79 <math>\pm</math> 0.02</b>	<b>0.79 <math>\pm</math> 0.03</b>	<b>0.80 <math>\pm</math> 0.04</b>
1963827	0.78 $\pm$ 0.03	<b>0.80 <math>\pm</math> 0.01</b>	<b>0.80 <math>\pm</math> 0.03</b>	<b>0.79 <math>\pm</math> 0.02</b>	<b>0.80 <math>\pm</math> 0.02</b>	<b>0.78 <math>\pm</math> 0.01</b>	0.76 $\pm$ 0.04	0.76 $\pm$ 0.03	0.77 $\pm$ 0.01	0.76 $\pm$ 0.02
1963831	<b>0.69 <math>\pm</math> 0.01</b>	<b>0.69 <math>\pm</math> 0.02</b>	0.69 $\pm$ 0.01	0.69 $\pm$ 0.02	0.68 $\pm$ 0.06	0.68 $\pm$ 0.02	0.68 $\pm$ 0.02	<b>0.70 <math>\pm</math> 0.02</b>	<b>0.71 <math>\pm</math> 0.03</b>	<b>0.72 <math>\pm</math> 0.05</b>
1963838	0.49 $\pm$ 0.01	0.49 $\pm$ 0.01	0.51 $\pm$ 0.04	<b>0.55 <math>\pm</math> 0.03</b>	nan	<b>0.54 <math>\pm</math> 0.02</b>	<b>0.53 <math>\pm</math> 0.01</b>	<b>0.55 <math>\pm</math> 0.02</b>	0.52 $\pm$ 0.04	nan